



Silk-Quality, Spinnability and Low Temperature Behavior

Fritz Vollrath
THE UNIVERSITY OF OXFORD

12/02/2015
Final Report

DISTRIBUTION A: Distribution approved for public release.

Air Force Research Laboratory
AF Office Of Scientific Research (AFOSR)/ RTB2
Arlington, Virginia 22203
Air Force Materiel Command

REPORT DOCUMENTATION PAGE				Form Approved OMB No. 0704-0188	
<p>The public reporting burden for this collection of information is estimated to average 1 hour per response, including the time for reviewing instructions, searching existing data sources, gathering and maintaining the data needed, and completing and reviewing the collection of information. Send comments regarding this burden estimate or any other aspect of this collection of information, including suggestions for reducing the burden, to Department of Defense, Executive Services, Directorate (0704-0188). Respondents should be aware that notwithstanding any other provision of law, no person shall be subject to any penalty for failing to comply with a collection of information if it does not display a currently valid OMB control number.</p> <p>PLEASE DO NOT RETURN YOUR FORM TO THE ABOVE ORGANIZATION.</p>					
1. REPORT DATE (DD-MM-YYYY) 03-12-2015		2. REPORT TYPE Final Performance		3. DATES COVERED (From - To) 01-06-2012 to 31-05-2015	
4. TITLE AND SUBTITLE Silk-Quality, Spinnability and Low Temperature Behaviour				5a. CONTRACT NUMBER	
				5b. GRANT NUMBER FA9550-12-1-0294	
				5c. PROGRAM ELEMENT NUMBER 61102F	
6. AUTHOR(S) Fritz Vollrath				5d. PROJECT NUMBER	
				5e. TASK NUMBER	
				5f. WORK UNIT NUMBER	
7. PERFORMING ORGANIZATION NAME(S) AND ADDRESS(ES) THE UNIVERSITY OF OXFORD UNIVERSITY OFFICES OXFORD, OX1 2JD GB				8. PERFORMING ORGANIZATION REPORT NUMBER	
9. SPONSORING/MONITORING AGENCY NAME(S) AND ADDRESS(ES) AF Office of Scientific Research 875 N. Randolph St. Room 3112 Arlington, VA 22203				10. SPONSOR/MONITOR'S ACRONYM(S) AFRL/AFOSR RTB2	
				11. SPONSOR/MONITOR'S REPORT NUMBER(S)	
12. DISTRIBUTION/AVAILABILITY STATEMENT A DISTRIBUTION UNLIMITED: PB Public Release					
13. SUPPLEMENTARY NOTES					
14. ABSTRACT <p>This project set out to measure, analyze and interpret as well as practically deploy the huge range in mechanical behaviour between different silk species and intra-species varieties. In particular, I set out to formulate a clear-cut link between a silks quality its internal structure and its consequent properties. Here two specific tracks were followed, namely thermal behaviour and melt behaviour. In addition, the uses of different silks in composites with designed properties were examined. The 1st research project (WP1) used thermal analytical methods to truth specific molecular signatures that allow us to differentiate silk qualities. Here thermal analytical methods were used to truth specific molecular signatures that allow us to differentiate silk qualities. For this, DMTA measurements were correlated with changes in molecular and morphological structure resulting from external factors such as diet rearing spinning conditions and storage</p>					
15. SUBJECT TERMS Biomaterials					
16. SECURITY CLASSIFICATION OF:			17. LIMITATION OF ABSTRACT UU	18. NUMBER OF PAGES	19a. NAME OF RESPONSIBLE PERSON Fritz Vollrath
a. REPORT Unclassified	b. ABSTRACT Unclassified	c. THIS PAGE Unclassified			19b. TELEPHONE NUMBER (Include area code) 44-1865-271234

Standard Form 298 (Rev. 8/98)
Prescribed by ANSI Std. Z39.18

DISTRIBUTION A: Distribution approved for public release.

SILK QUALITY, SPINNABILITY AND LOW TEMPERATURE BEHAVIOUR.

PROF FRITZ VOLLRATH

DEPARTMENT OF ZOOLOGY, UNIVERSITY OF OXFORD, OX1 3PS, UK

Scientific Progress Report 3rd yr (June 2014-May 2015) and overall for 3 yr grant period

This project set out to measure, analyze and interpret as well as practically deploy the huge range in mechanical behavior between different silk ‘species’ and ‘intra-species varieties’. In particular I planned in this project to formulate a clear-cut link between a silk’s quality, its internal structure, and its consequent properties. In this part of our research we are following two specific tracks namely thermal behavior and melt behavior. In addition we are examining the uses of different silks in composites with designed properties

The 1st research project (WP1) examined thermal analytical methods to truth specific molecular signatures that allow us to differentiate silk qualities. Here we used thermal analytical methods to truth specific molecular signatures that allow us to differentiate silk qualities. For this we correlated DMTA measurements with changes in molecular and morphological structure resulting from external factors such as diet, rearing, spinning conditions and storage. We examined whether and how these quality factors propagate into property changes also in reconditioned silks.

The 2nd research project (WP2) examined how silks spun under controlled conditions behave, and what this might tell us about the natural spinning process, and attempts at artificial spinnerets. Here we examined how unspun native silks can behave like melts, while reconstituted silks are solutions or suspensions to test the hypothesis that this is the key difference between the two types of material. Techniques used were rheometry as well as investigations of biological and artificial silk extrusion spinning processes.

The 3rd research project (WP3) aimed to make and test silk composites made from silks of different material quality and evaluate structure-properties relationships. Here we aimed specifically to develop sustainable silk-reinforced biocomposites, in the form of textile laminates, syntactic foams and sandwich-structures, and critically evaluate their performance (mechanical, thermal, environmental) in comparison to conventional materials. To facilitate this project and to provide novel insights from natural composites we also conducted fundamental characterization studies on various natural biocomposites and biopolymers, such as the tube housing of a polychaete marine worm, elephant ivory and native plant latex, for inspiration on the design and fabrication of novel functional, bio-inspired materials.

Results from the 3rd yr studies are integrated into the overall project report, with the **Figures relevant to results from yr3 highlighted in grey.**

General Overview and Summary Introduction to Project

Silk is an important material, both academically and commercially, and the Oxford Silk Research Group offers a solid combination of access to the relevant natural materials, analytical equipment and modelling tools as well as the skills to achieve the very ambitious goals set out in this proposal. Summarising the three goals of the AFOSR funded research: (i) unravel the ‘quality’

characteristics of benchmark silks, (ii) analyse the key ‘flow’ differences between native and reconstituted silks and, finally, (iii) develop and study silk composites.

WP (1): Analysis of Silk Quality

Dynamic Mechanical Thermal Analysis (DMTA) We were able to demonstrate that DMTA is able to identify specific molecular signatures in silks. This allows us to differentiate high quality from low quality silks, which is making DMTA a potentially very effective tool for evaluating “quality” and variability in silks. This has both commercial and academic implications. In our pilot case study (outlined in the proposal) we examined three cocoon silk grades (G1, G2 and G3) from the same region in China during the same period of production and discovering statistical differences in the mechanical properties of three grades. We further discovered that lower grade silks display lower temperature glass transitions, which are characteristic of different types of molecular structure in the disordered phase. Interestingly, the temperature annealing treatment under load can “heal” these poor silk structures and reduce the differences between the poor and good silks.

Hypothesis: Specifically, the loss peaks observed by DMTA in the glass transition region of silks 150-220 °C have a clear relation to specific types of disordered structure with different conformations and degrees of hydrogen bonding, which also determine mechanical properties. These structures are determined by production and processing conditions of the silk.

Key reference: Thermally Induced Changes in Dynamic Mechanical Properties of Native Silks, J. Guan, D. Porter, F. Vollrath, *Biomacromolecules* 2013, **14**, 930–937

The basis of our hypothesis is shown schematically in Figure 1.1 as a DMTA loss tangent plot through a typical temperature scans on a silk. First, a temperature scan (red line) up to about 160°C shows two main types of feature: (1) low temperature peaks associated with relaxation of hydrated silk at about -60°C and a second peak due to water evaporation from the silk at about +60°C; (2) higher temperature and magnitude peaks associated with the glass transition of disordered silk structures, usually in the range 150-220°C. Second, a repeat temperature scan (blue line) shows that the water peaks have disappeared and the T_g peak may shift to a higher temperature, showing that the first scan essentially annealed the silk into a new structure.

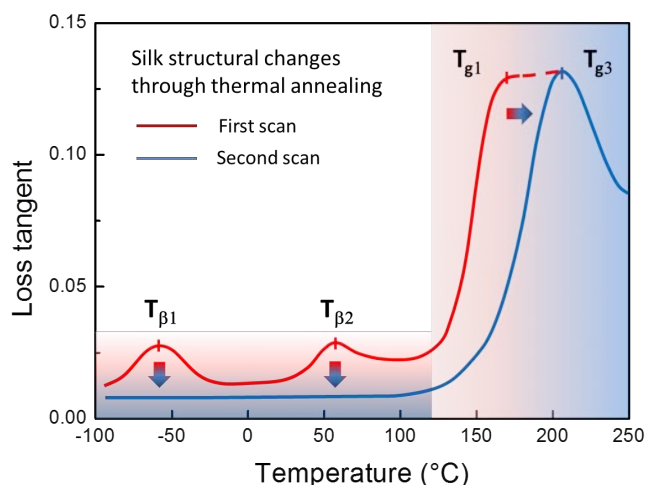


Figure 1.1. Schematic DMTA temperature scans showing the main loss profile features of a typical silk fiber. The first scan (red) shows low temperature peaks associated with water-silk interactions and higher

temperature peaks associated with glass transition events. After cooling and reheating (blue), the water features are lost and the T_g peak shifts to higher temperatures characteristic of anneal structures with a better hydrogen bonded molecular packing.

Figure 1.2 shows that silk 'quality' can be clearly identified by the higher temperature loss profile. Figure 1.2a compares three different commercially graded silk fibers (grades 1, 2, and 3), where the lower grade or quality silks have a number of lower temperature loss peaks below the limiting 'best' quality peak at about 220°C. Figure 1.2b shows results for silks deliberately produced as 'bad' silks under poor conditions of rearing and production, again with multiple loss peaks that we have identified as discrete features with a clear structural identity. Figure 1.2c then shows that a poor grade 3 silk can be 'annealed' by stretching the fibers as they go through the lower temperature relaxation events that allow some degree of molecular mobility.

We have quantitatively related the lower temperature T_g loss peaks to structure in the disordered phase in terms of numbers of hydrogen bonds and restrictions on the chain backbone vibrations. Most specifically, the 150°C peak has only one hydrogen bond, the 175°C peak is the standard RSF silk disorder, and the limiting 220°C peak has chain restrictions due to hindrance.

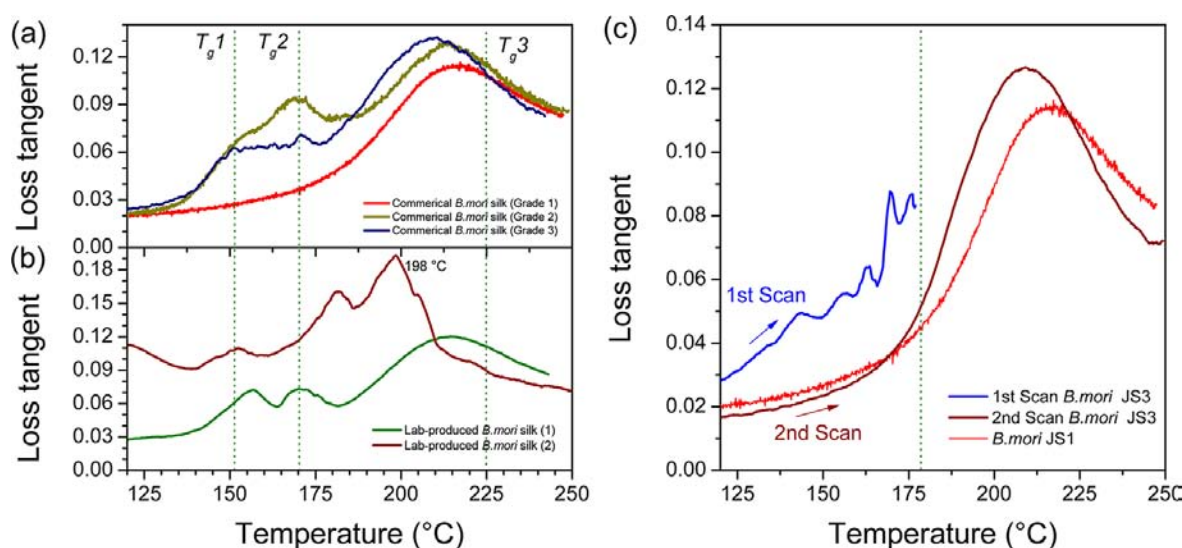


Figure 1.2. DMTA plots showing that the variability of different silks can be identified: loss tangent profiles from three different grades of commercial silks all reared under the same conditions (a), two lab-produced 'poor' silks deliberately produced under bad conditions (b), and grade 3 silk before/after annealing to 180 °C compared with one scan of grade 1 silk (c).

The disordered structures identified by DMTA control mechanical properties is shown in Figure 1.3, where DMTA annealing at 120°C changes the engineering stress-strain profile, even in a good quality silk. Clearly, this is due mainly to removal of water in this case, but ongoing work with higher temperature annealing up to 180°C shows similar effects.

The next stages of the work are underway, where deliberately created 'bad' silks with different production conditions are being tested using DMTA and mechanical tests. The objective here is to make clear relations between the protein secondary structures in the disordered phase and the observed mechanical properties, and to find tools to control these structure through post-treatment of silk fibers to ensure consistent and high quality materials for future application. In particular, we are investigating force reeled silks with different post drawing treatments and on the analysis front we will use different chemical, humidity and temperature combinations on the DMTA to clearly differentiate the structure and function of the different structures.

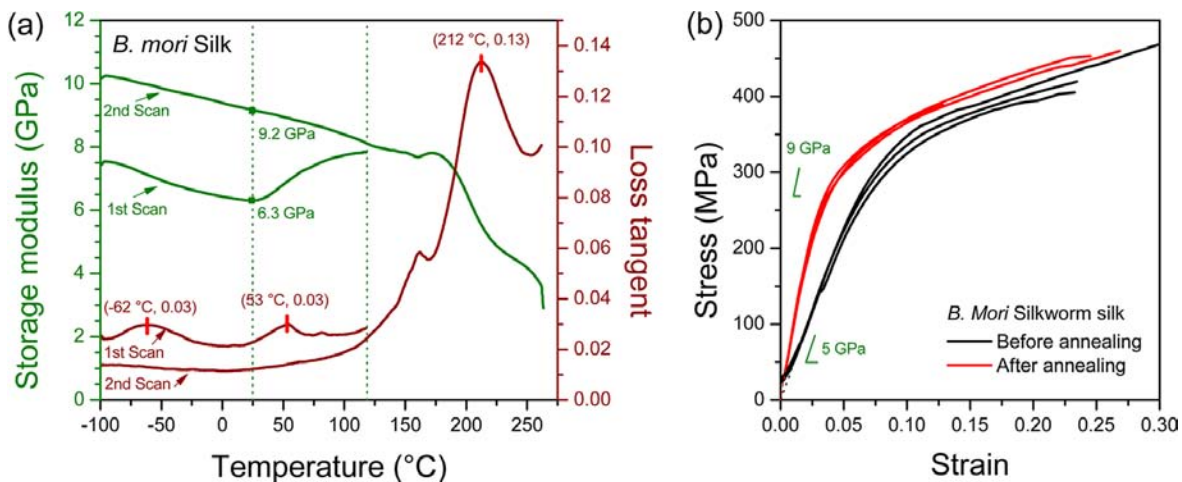


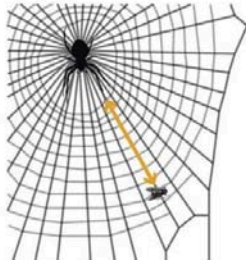
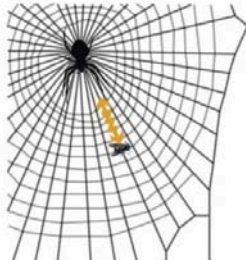
Figure 1.3. The effect of annealing at 120°C on the mechanical properties of silk. The removal of loss peaks essentially stiffens the silk fibres at low strain due to the loss of plasticizing water in the annealing process.

We conclude that DMTA can be used to study silk quality and also to monitor improvements performed by processes such as annealing.

High Rate Impact

In order to study, in more detail, the internal properties of silks we developed and deployed High-rate Impact techniques with first results giving interesting and important insights.

Table 1. Summary of findings.

	Longitudinal	Transverse
Wavespeed variation between materials	Governed by storage modulus	Does not vary between polymers as densities and response to tension is similar
Wavespeed sensitivity	Storage modulus, (slight effect of tension), (slight effect of frequency) ^{a)}	Tension, (slight effect of frequency) ^{b)}
Resonance sensitivity ^{b)}	Distribution of structures in the material	Fiber number, fiber diameter, distribution of structures in the material
Hypothesised use in web	Vibration propagation of all kinds, where any resonance will be above 1kHz	Web condition signals, resonance at short silk lengths from silk plucking
		

Overview of high-rate ballistic impact findings

A well established transverse wave propagation technique was applied to the problem of characterising the high- rate material response of *Bombyx mori* cocoon silk and medium tenacity nylon. Our approach has the benefit of being an intrinsically non equilibrium approach to deriving mechanical response, so does not have the limitations of the Hopkinson bar in obtaining high-rate, low strain data. The technique can also be readily extended to derive spatially-resolved strain data by applying a pattern to the specimen fibre, and as only the central 20cm span of the fibre are relevant to the experiment, environmental controls are easily implemented on this short section.

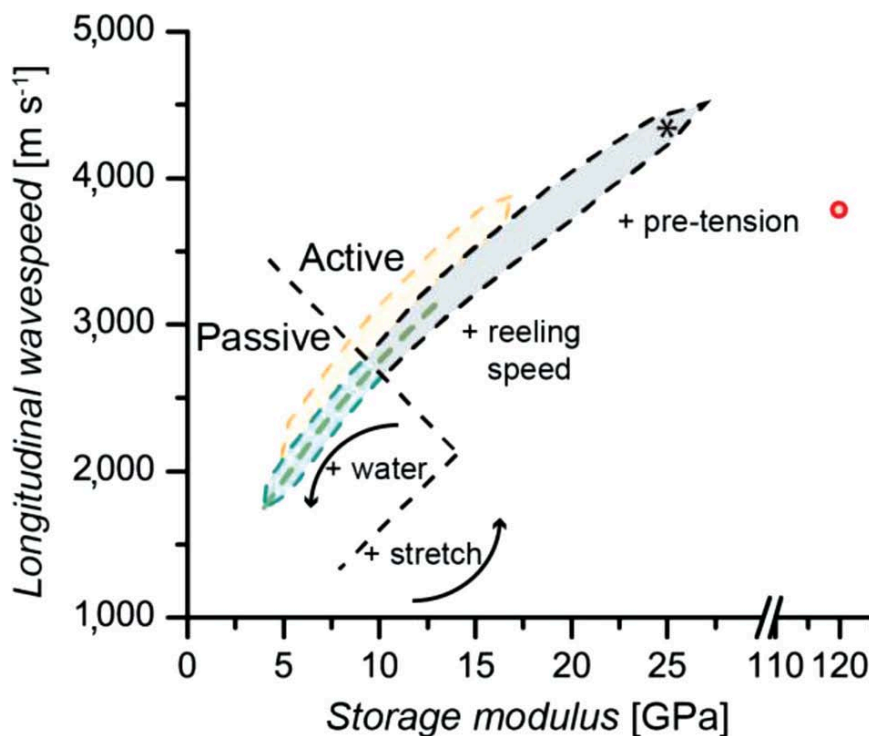


Figure 1.4 Storage modulus versus longitudinal wavespeed for different materials. Polymers and silks follow a (root) dashed line, [18] so shaded area is given to allow different materials to be distinguished. Metal wire has a single coordinate. Materials: copper beryllium wire (red), silkworm silk (dark green dashed line), nylon (orange), *Nephila* major ampullate spider silk (dry: black, wet: cyan). Asterisk gives low tension, dry Aciniform spider silk. [33] For the major ampullate silks, wavespeed can change with passive and active controls: for the former, wetting the silk allows supercontraction, lowering modulus; in the latter, modulus can be altered by processing conditions such as reeling speed, but also by applying tension or stretching, which increases the storage modulus to the highest levels measured.

Furthermore, we employed two means to access the high rate behaviour of individual fibres — a velocity-varying approach, which seeks to fit a stress–strain curve to experimental (V, CW) data; and the pre-stress varying approach, where the fibre was statically loaded to various pre-stress states prior to impact, and elastic wave theory was used to calculate the resulting increase in stress and strain. Importantly, both techniques produced identical impact stress–strain curves for silk, but not for nylon. This is explained by the differing micro- and nano-structure of these semi-crystalline fibres, which affects their ability to share strain energy between the ordered and disordered domains. It is also noted that the high-rate stress–strain curves derived for silk illustrate superior energy absorption to nylon, and the energy imparted by the passage of a longitudinal wave varies little with pre-stress. Together this suggests that the millions of years of natural selection acting upon silks has resulted in optimisations for superior toughness at both low and high rates, attesting to the fact that there are still many more lessons to be learned from nature.

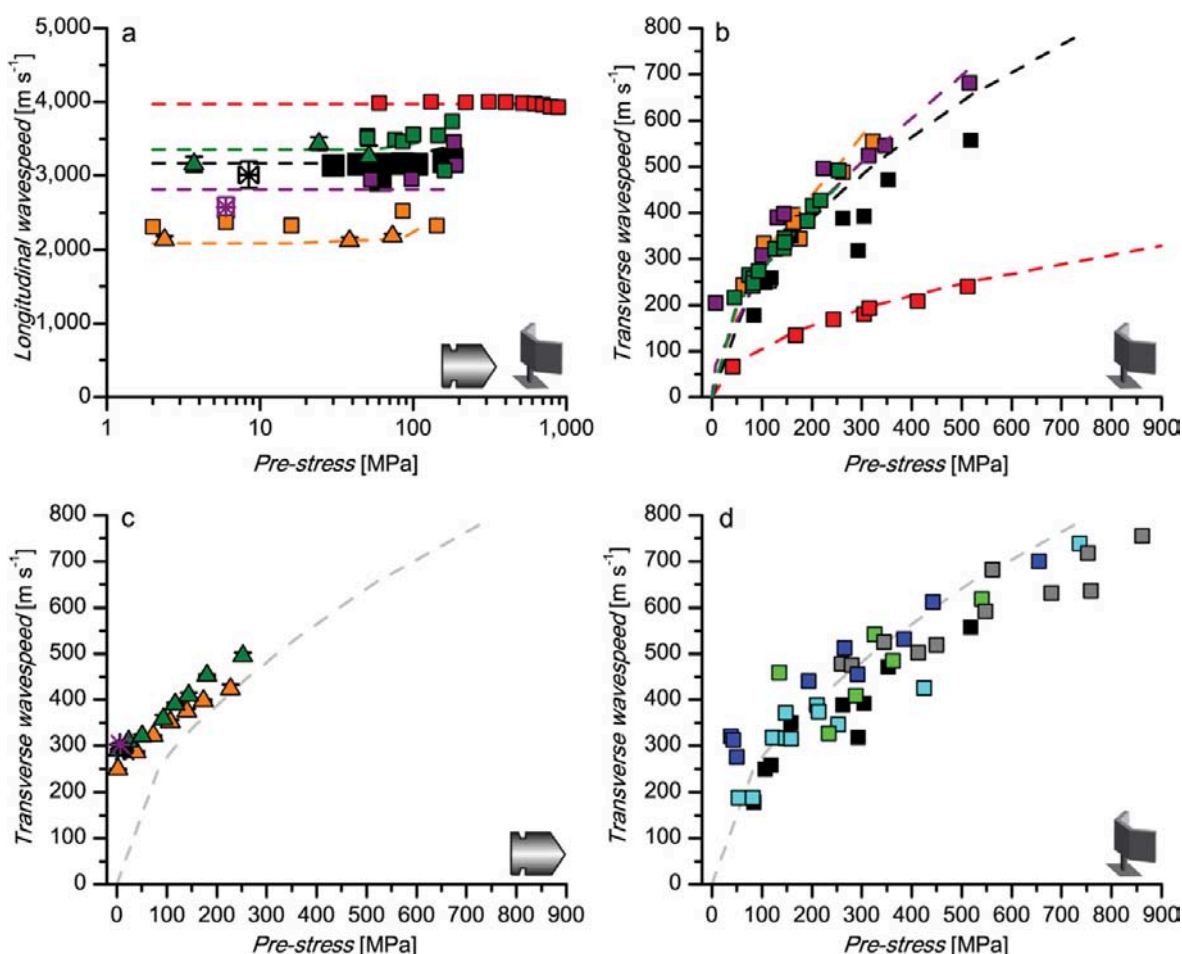


Figure 1.5 Wavespeed as a function of pre-stress. a) Longitudinal wavespeed (log axis) and b)-d) transverse wavespeed. Theoretical calculations are given by dashed lines, vibrometry data (shown by speaker symbol) by squares, ballistic impact data (shown by bullet symbol) for spider silks at low tensions and 220 m s^{-1} by stars and data adapted from Drodge *et al.* by triangles. Ballistic impact data include standard error of the mean bars, for both wavespeed and pre-stress for spider silks, and wavespeed for nylon and silkworm silk as pre-stress was consistent between repeats. Acoustic measurements do not have error bars as they are all individual samples. Materials: copper beryllium wire (red), silkworm silk (dark green), nylon (orange), *Nephila* major ampullate (MA) spider silk (big size, black; small size, dark grey; small size supercontracted, blue), *Nephila* minor ampullate (MiA) spider silk (purple), mixture of *Nephila* silks (2 MA, 2 MiA: cyan), and *Araneus* spider bundle (2 MA, 2 MiA: green). For b) and c), the grey dashed line gives a reference spider silk theoretical curve.

WP (2): Analysis of native and recon Silk Melts and Dopes including bio-spinning

Silks form a unique class of natural polymer fabricated in a solvent-spinning process (fundamentally familiar to industry). This process has evolved several times independently and, importantly for us, is accessible to laboratory investigation. Research led us towards a major shift in our understanding of the molecular-level mechanisms that control the rheological properties of silks as opposed to non-silks, including silk fibres that have been reconstituted into solution form. This led to the formulation of the *aquamelt*, which is based on original research that uses techniques and models used to study synthetic polymers. We conclude that native silk polymer molecules behave like aqueous liquid crystal elastomers, which flow as ‘strings’ of coiled polymeric beads. Importantly, native silk molecules and their associated water must be considered to be a *single processable entity*, an “aquamelt”, which thus (much like an individual

polymer chain in a melt) is a nanostructured state of biological matter.

Hypothesis: Specifically, the rheological properties of natural silks and their energetically efficient processing hinges on the ability of a native silk protein to carefully control its conformation and interaction with its bound water during denaturation. Generically, understanding the energetics of the spinning process via rheology will lead to utilising novel ultra-low energy processing routes to produce nanoscale, hierarchically organised structures either form either reconstituted or synthetic polymeric materials.

The basis of this work is our previous observations that compare the very different rheological properties of native and recon silk solutions [Chris references]. While simple accepting that native silk solutions have much higher viscosity and can thereby more effectively induce macromolecular alignment and subsequently better solid fibre properties, the broader scope of our work suggested that native and reconstituted silks are fundamentally different at the electronic structure level in the same way that any 'live' protein differs from materials derived by reconstitution of 'dead' or denatured protein. So, the initial phase of this program of work is to understand what these differences in structure are, and use this understanding in our attempts to produce larger quantities of silk solutions for subsequent processing that have the positive attributes of native silk without the need to dissect the native material from a live creature.

The first step was to understand the process of denaturation in proteins, and simple proteins like silk in particular. To do this, we previously used *ab initio* quantum mechanics simulations of water-peptide interaction to quantify the instability conditions under which the water become mobile relative to the protein chains and allows either the chains to randomise and lose function or to aggregate into insoluble semicrystalline solids (such as silk fibres) [references]. This fundamental understanding of denaturation can be applied to any protein and is generally very significant, but specifically for silks, it allowed us to understand quantitatively the combination of environmental (temperature, pH, and mechanical) stresses that can induce the phase change from silk dope solution for solid fibre.

The more recent model [BBAPAP ref] also allowed the frequency effects of some of the relaxation processes in protein solutions to be understood and predicted quantitatively, as shown in Figure 2.2, but these processes are essentially only valid for the denatured (in silk reconstituted) random configuration of proteins, but not for the stronger enhanced hydrogen bonding of the water-peptide interaction that we need for native proteins such as silks. So, we needed to look at the fundamental dynamics of water-protein interactions at the electronic structure level to try to understand the 'aquamelt' rheology.

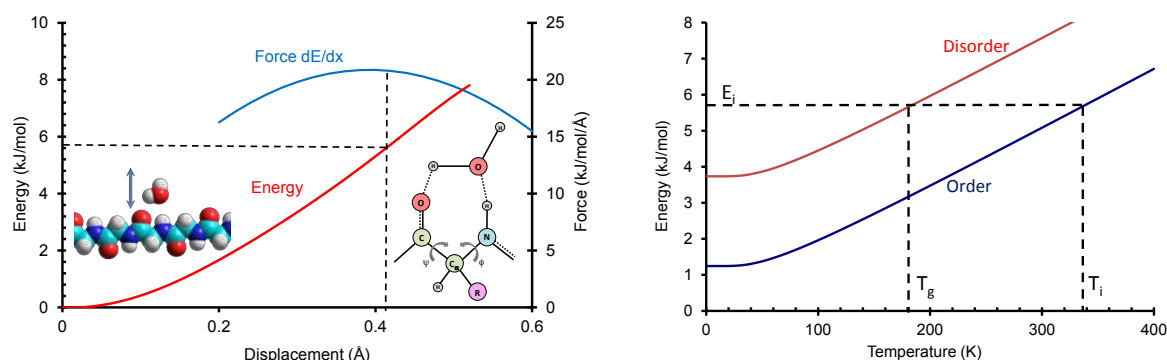


Figure 2.1 Model for the instability of water-protein interactions. (a) energy condition for interaction instability at the Born elastic instability condition of a maximum in intermolecular force that corresponds to zero bond stiffness. (b) Translation of the instability energy to temperature (using heat capacity models to convert heat energy into temperature) for both disordered (T_g condition) and ordered (denaturation)

interactions.

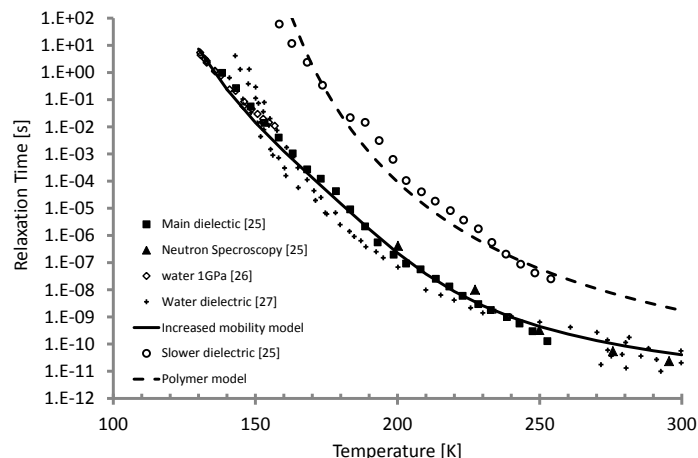


Figure 2.2. Predicted relaxation times for disordered water-silk interactions compared with experimental observations. The two curves for slower (upper) and faster (upper) relaxation time are attributed to the local water and macromolecular chain relaxation processes respectively.

Very recent work [new Soft Matter 2013] shows how we used quantum dynamics simulations to show that proton hopping within the relatively stable water-peptide bonded structure is responsible for the key electronic and dynamic relaxation properties of 'live' proteins. A snapshot of a proton hopping structure simulation is shown in Figure 2.3 to illustrate the process of proton hopping both along and between protein chains.

We were able to predict the nature and the relaxation times (such as temperature dependence) of the hopping process for electronic activity in proteins that will be the basis of our new rheological property framework. This mechanism is fundamentally different from simple polymer or denatured protein solutions, in that the water is an integral part of the whole protein-water complex at the electronic structure level; exactly as per the 'aquamelt' hypothesis from rheological observations. While this new insight may have important implications for protein electronics, etcetera, a more practical use of this mechanism is that it points into some new directions for the reconstitution process for producing silk solution that have the same characteristics as native silks.

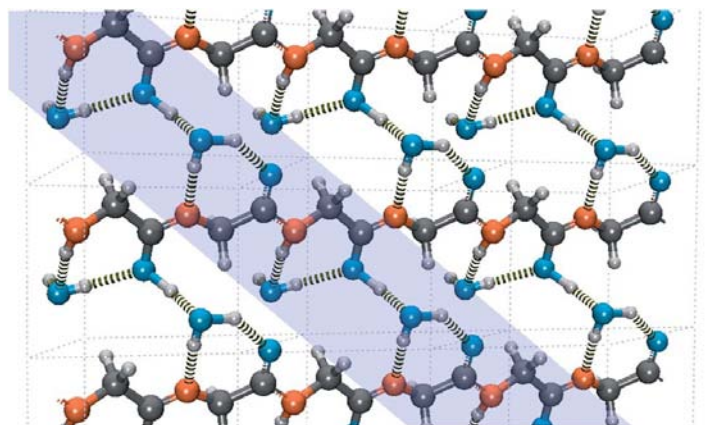


Figure 2.3. A snapshot of a proton hopping dynamics simulation, where protons (blue hydrogen atoms) move both along and between protein molecular chains with fluctuations in the hydrogen bonding (shown

as dashed lines between atoms).

Developing Differential Scanning Fluorimetry

We conclude that fundamental research on the role of water will be key to understanding not only the formation but also the properties of silks. To study this fundamental question experimentally we modified the technical paradigm of real-time PCR (polymer chain reaction) to study protein transitions. This technique uses Differential Scanning Fluorimetry (DSF) and allowed us to probe small quantities of valuable silk samples in great detail.

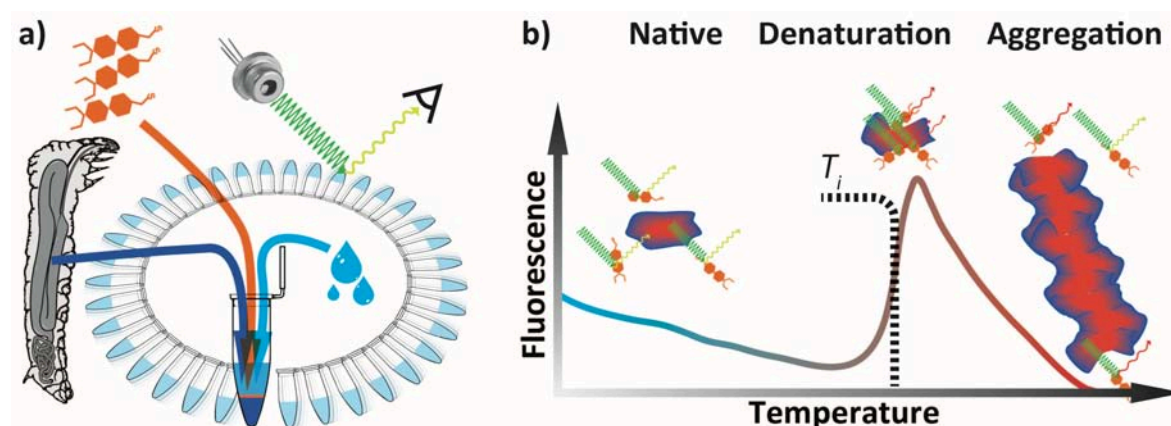


Figure 2.4 Differential Scanning Fluorimetry (DSF) aka Thermofluor Assay aka Thermal Shift, Assay technique and signal. (a) Schematics illustrating the sample preparation for high, throughput dynamic scanning fluorimetry thermal stability assay (b) Cartoon representing the, native, denatured and aggregated states of protein alongside its typical exogenous, fluorescence response.

To study in detail the thermal transitions of silk proteins (over a biological range) we used a state-of-the-art a real-time quantitative polymerase chain reaction (qPCR) instrument as it can automatically process many controlled conditions and interactions in a single run, allowing us very cost efficiently process hundreds of trials in a day. The technology, never before tried to probe fibrous protein denaturation transitions relies on a thermofluor assay or thermal shift assay whereby a ligand e.g. a dye begins to fluoresce as it binds. Our experiments show that Differential Scanning Fluorimetry (DSF) is a true high throughput screening method for silk solutions that probes the refolding of the protein as it experiences progressive denaturation. The technique relies on using specific dyes that fluoresce as they interact with proteins in their denaturation transition between a strongly hydrated solvated state and the final aggregated solid state. It allows us to investigate the folding of the silk protein molecules as they abandon their first native melt conformation, dehydrate and denature into their final solid filament conformation. Our first data and analyses comparing silks from spiders, mulberry and wild silkworms as well as reconstituted 'silk' fibroin show that DSF can provide valuable insights into details of silk denaturation processes that might be active during spinning.

In addition to its features of high throughput and low costs, DSF technology has led to the development of a wide variety of specific exogenous fluorescent molecules, which makes it an extremely versatile technique. In a typical application, temperature transitions are used to probe the interactions of a protein with a fluorescent dye as it binds with specific sites such as residues exposed during unfolding. Sypro® orange is well suited as dye of choice as it was designed specifically to activate fluorescence when binding to hydrophobic patches exposed as a result of conformational changes. Using such a specific dye, DSF elicits and identifies key

temperature transitions and protein stability features, which in turn allows the probing and analysis of molecular interactions. Other dyes designed to bind to hydrophobic regions of amyloid fibrils might also be of interest because silk and amyloid fibrils share important folding characteristics. Moreover, highly specific antibodies with labels such as the green fluorescent protein (GFP) could also be used with DSF in order to target specific domains of a protein.

Silk is a perfect model material for the study of protein denaturation. Firstly, Nature has evolved many thousands of silks, which between them sport many minor as well as major sequence differences in addition to displaying key differences in processing (i.e. dehydration/denaturation) parameters. Secondly, unlike most other proteins, silk proteins have evolved to denature 'on demand' in order to assume their 3rd functional 'state' i.e. that of a thread. A silk's 1st state has the molecule in its long-term storage conformation. Its 2nd state occurs during the rapid structural reconfiguration during spinning. This three state transition progress is genetically pre-programmed, which makes silk protein conformation transitions interesting and valuable generic research tools. For example, there is overlap with amyloid formation yet in the case of silks this is not an errant 'mis'-folding pathway but the result of design by evolution. One could consider the 1st state to be classed as active (alive) - for the protein molecules stored in the gland are labile and easily denatured if perturbed. The 2nd state could be called re-active - for each molecule refolds and reconfigures according to the environmental conditions it experiences in the controlled environment of the spinning duct. And the 3rd state could be deemed inactive (dead) - for the denatured protein molecules no longer respond actively as individuals to environmental conditions. Instead, they are now firmly locked into a polymer network, responding passively and collectively to stresses and strains imparted on the bulk material. Whether one agrees with this view or not, it is well established that silk molecules have two different states linked by a distinct, one-way transition. We may assume that 400M years of selective tweaking and tuning will have evolved a 'spinning' process that is highly advanced. The three major independent evolutionary pathways (in insects, arachnids and crustaceans³⁶) that have led to more or less the same proteins and processes suggest to us that silks can provide insights into protein denaturation that are likely to be generic.

We conclude that this technique and technology novel to silk studies provides a powerful and new tool to analyse silk protein transitions in detail by allowing many changes to the silk solutions to be tested rapidly with microliter scale sample sizes. Such transition mechanisms will provide important generic insights into the folding patterns not only of silks but also of other fibrous protein (bio)polymers.

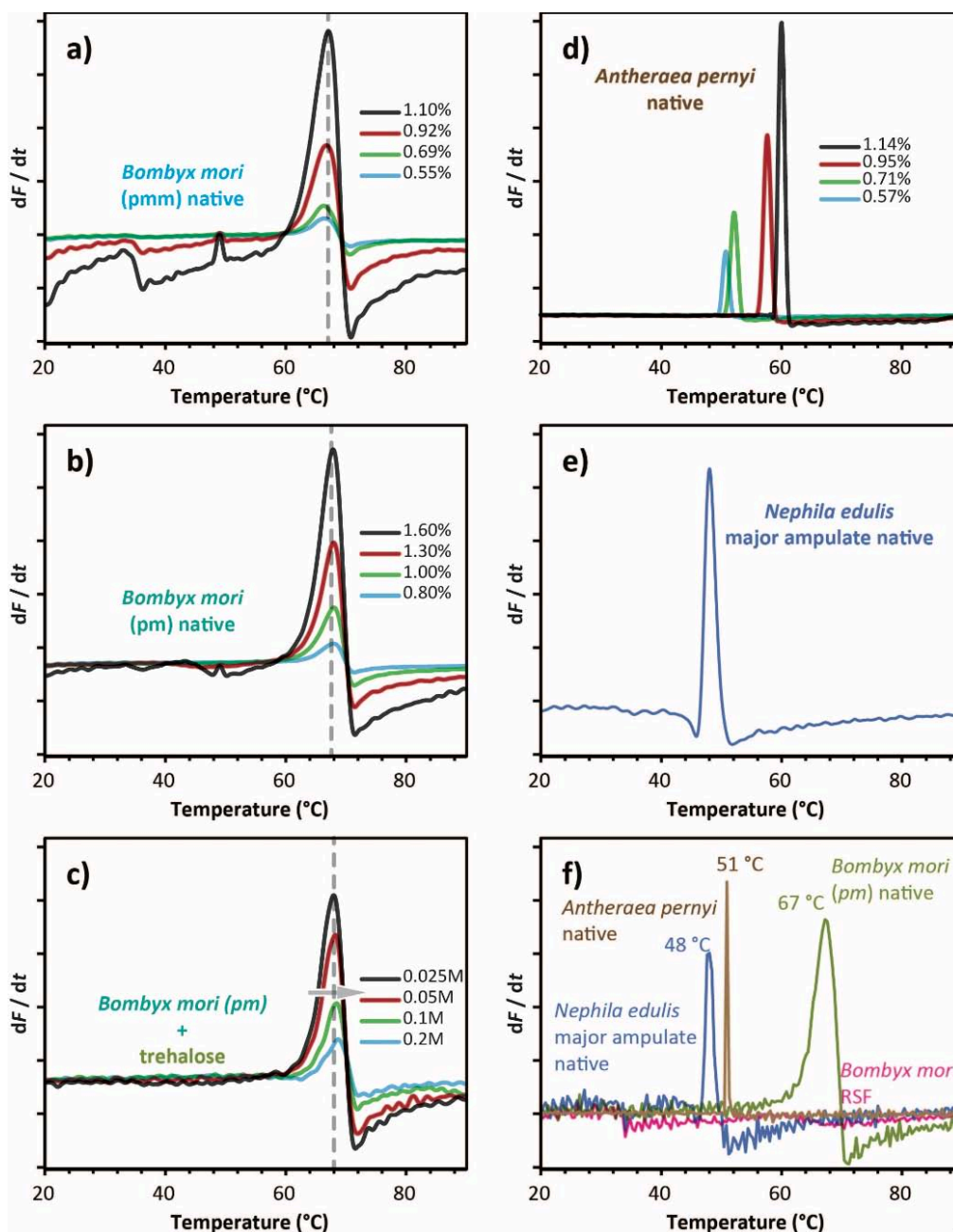


Figure 2.5 DSF fluorescence signals of various silks feedstock/dopes and dope, concentrations. (a, b) For the ‘domesticated’ silk of *Bombyx mori* the signal decreases in, strength as a function of silk dope concentration for two distinct major parts of the gland, (pmm for middle section and pm for posterior section, details in SM). (c) For the ‘wild’ silk of, *Antheraea pernyi* the picture is rather different with the signal shifting not only changing in, strength but also shifting along the temperature ramp as a function of dope concentration. (d), The signals for dope from the Major Ampullate gland of the *Nephila edulis* spider resemble, those for *Antheraea* dopes at high concentration. (e) Trehalose affects the signal of *Bombyx*, dope (shown by the arrow) dependent on the concentration of the additive. (f) Overlay of the, exogenous fluorescence intensity first derivative for native dope of *Bombyx*, *Nephila* and, *Antheraea* as well as for reconstituted silk dope made using *Bombyx* silk fibres.

Fundamental understanding of Specialist Silks and Natural Spinning Processes.

This research project (WP2) within the overall AFOSR funded programme examines how silks spun under controlled conditions behave, and what this might tell us about the natural spinning process, and attempts at artificial spinnerets.

Importantly, we believe, we discovered and localized chitin in the cuticle of the spinning ducts of both the spider *Nephila edulis* and the silkworm *Bombyx mori*. These observations demonstrate that the duct walls of both animals contain chitin notwithstanding totally independent evolutionary pathways of the systems. We conclude that chitin may well be an essential component for the construction of spinning ducts; we further conclude that in both species chitin may indicate the evolutionary origin of the spinning ducts. This leads us to the further conclusion that the surface covering of the spinning duct is likely to play an important role.

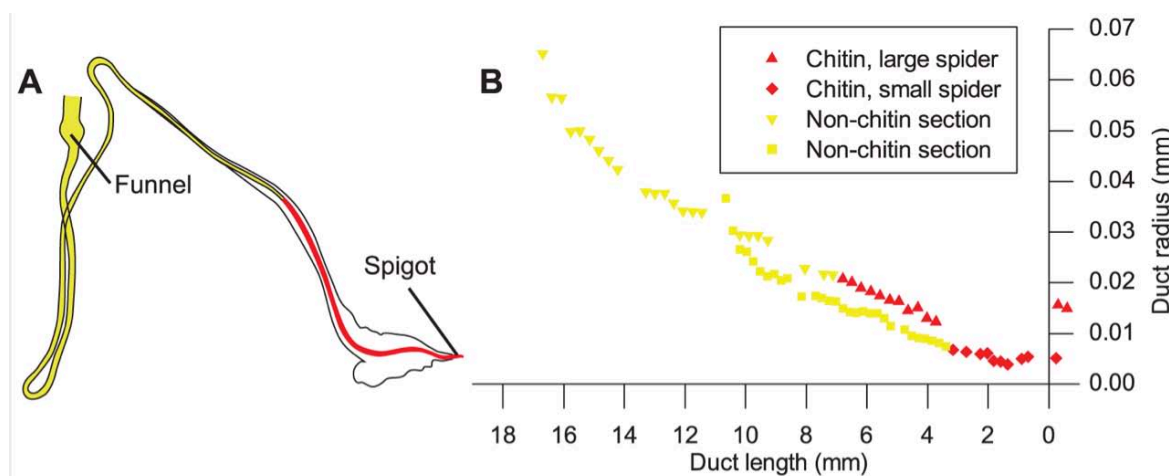


Figure 2.6 Chitin location within the spider duct. (A) Tracing of spider duct, showing portion solubilised by acid in yellow and section remaining after KOH treatment and testing positive for chitin highlighted in red. (B) Duct profile of both early and late spider instars from Figure 2 in Davies, Knight et al. 2013, with valve positioned at $x=0$. The symbols (red diamonds early instar; red triangles late instar) are for the part of the duct that stains for chitin and the yellow from the remainder of the duct that is destroyed in the test. This indicates that the surviving region is confined to the section of the duct that narrows linearly in both early and late instar spiders.

In addition to this work we continued to explore the nano-scale spinning ducts of the cribellate spiders. Here we discovered what we believe is a spinning system novel for spiders, and are following up more detailed studies, which however are turning out to be rather tricky due to the small scale of the set-up.

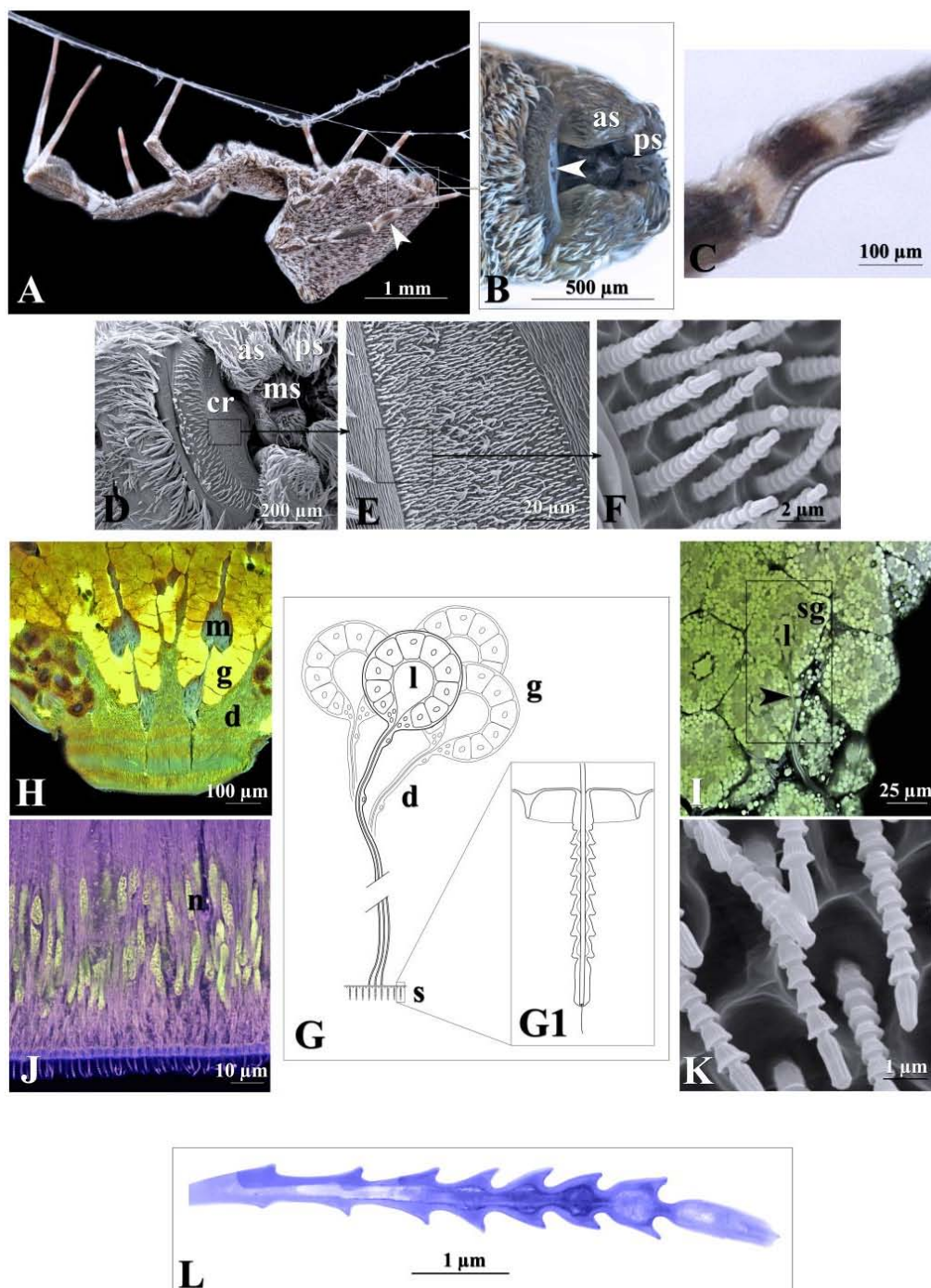


Figure 2.7 The Cribellum of *Uloborus plumipes* (adult, ♀). (A) *Uloborus plumipes* in lateral view; arrowhead indicates the position of the setal brush on the metatarsus of the fourth leg used to brush out the cribellum catching wool. (B) The spinning apparatus with spinnerets in inactive position; arrowhead indicates the cribellum. (C) Calamistrum, the hackling comb. (D-F and K) SEM images of the Cribellum spinning field and spigots. (H-I) TEM cross sections of the system, length-wise (H,J) and cross-wise (I). (G) Schematic of the system. (L) cross section of a spigot showing the highly unusual morphology.

Nanometre scale ribbons of strong high-quality silk film: We introduced a totally novel thin-film materials system to the wider science community. The remarkable silk of this spider (so well known for its toxins) combines the best properties of a dragline silk with a unique morphology. In contrast to other silk fibres recluse silk is a flat ribbon with a thickness of only a few ten

nanometres. Thus, recluse silk is both a fibre and a very thin biopolymer film. Importantly, this allows us to study the essence of a spider silk as we now can deploy analytical tools not appropriate for the typical spider silk which is always cylindrical with a skin-core morphology. Moreover, this naturally evolved material allows us to test the properties of super-thin silk films, which are often envisioned as potential platforms for a range of applications in e.g. regenerative medicine or electronic devices. Currently there simply is no other way of spinning silks with similar morphology to the high standards achieved by the spider itself. We believe this to be a great example for bio-inspiration.

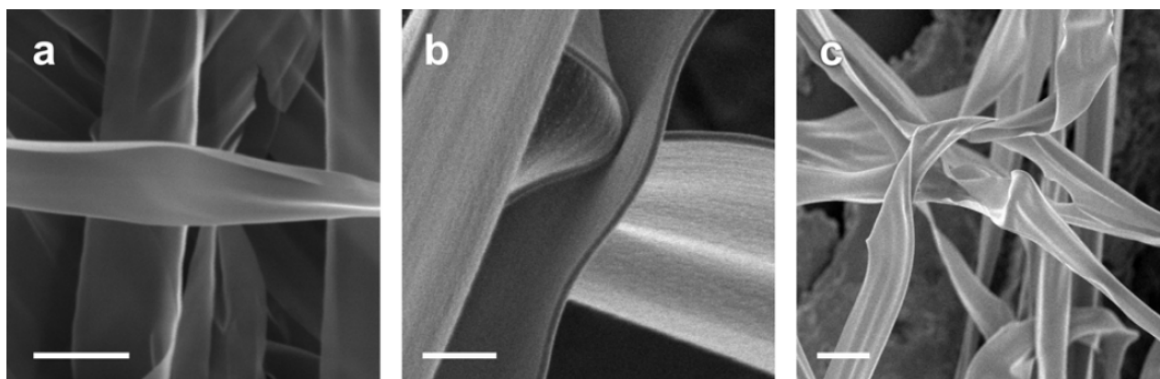


Figure 2.8 The ribbons of the *Loxosceles* spider have an aspect ratio of 100:1 and above. (a) Scanning electron micrograph (SEM) featuring several ribbons (scale bar: 5 μm). (b) Side view showing the thinness of the ribbon (scale bar: 500 nm). (c) Due to their thinness, the fibres bend and wrinkle easily (scale bar: 5 μm).

The silk from the *Loxosceles* spider features a unique, ribbon-like morphology unlike any other spider silk or synthetically spun polymer fibre (Fig 1.4). These fibres can be extracted from the animals under controlled condition. They are ribbons that represent free-standing polymer films with a thickness of about 50 nm, corresponding to only a few molecular layers of protein, thus approaching a 2D polymer that is dominated by surface rather than bulk properties. Their thinness allows these fibres to bend and wrinkle easily, which promises interesting adhesive properties due to facilitated surface conformation to contacted objects. Due to its relative structural simplicity, this material is an ideal model system to study silk.

Using an atomic force microscope we carried out stress-strain analysis of individual fibres (Fig 1.5). These were found to be fully elastic for strains of $\leq 1\%$ with a corresponding Young's modulus as high as 19 ± 5 GPa. Specifically we carried out our mechanical characterization of these nano-ribbons using scanning probe techniques. We believe that this 'loxo-silk' could become a benchmark for molecule-thin polymer films.

We conclude that this highly unusual silk system will inspire many scientists to explore the research opportunities provided by this material and its remarkable production system.

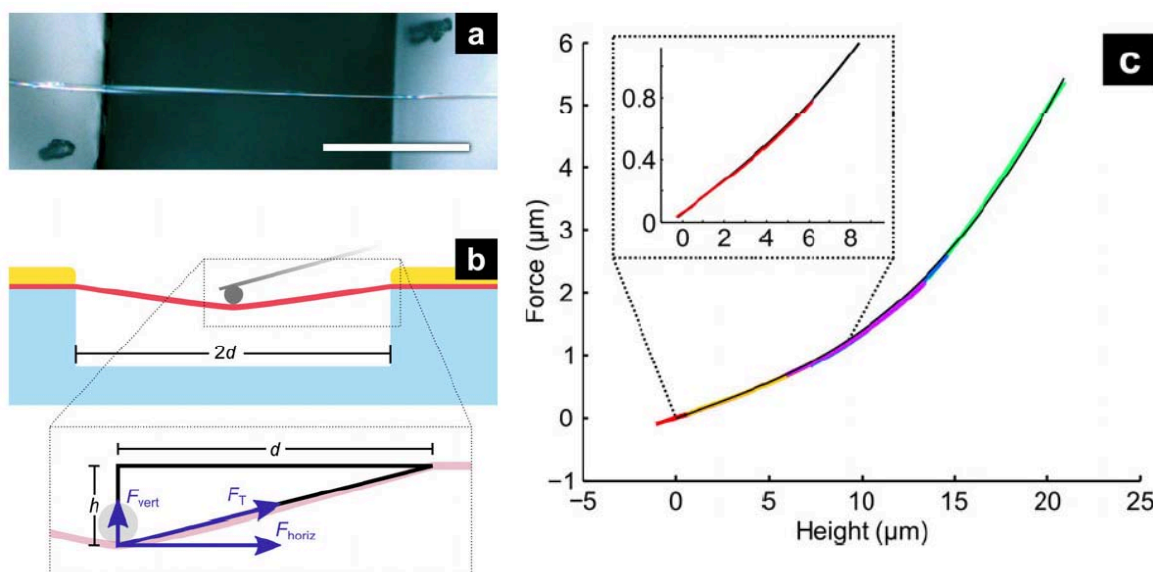


Figure 2.9 Mechanical testing experiment. (a) Top view of the mechanical testing setup (optical micrograph). Scale bar: 200 μm . (b) Schematic: A *Loxosceles* fibre (rose) was suspended over a gap in a glass substrate (light blue) and secured with cyanoacrylate glue (amber). A blunted AFM probe (grey) strained the silk via vertical deflection, while simultaneously measuring the vertical component F_{vert} of the fibre tensile force F_T as a function of the probe indentation height h . (c) Obtained force curves (various colours) and the fitted model (black).

Effect of charges

Clearly, electric charges play a great role in spider webs and silks. In order to get a better understanding of their action, we studied a range of webs where silks seemed to be attracted to charged objects. The glue-coated and wet capture spiral of the orb web of the garden cross spider *Araneus diadematus* is suspended between the dry silk radial and web frame threads. In this study we experimentally demonstrated that the capture spiral is electrically conductive because of necks of liquid connecting the droplets even if the thread is stretched. We examined how this conductivity of the capture spiral may lead to entrapment of charged airborne particles such as pollen, spray droplets and even insects. We further described and modeled how the conducting spiral will also locally distort the Earth's ambient electric field.



Figure 2.10 The distortion of an orb web of *A. diadematus* by a charged metallic sphere of radius 5 mm with voltages of +1 kV and -1 kV. In (a) the voltage is positive and in (b) it is negative demonstrating that the neutral but electricity-conducting web is equally attracted to the charged sphere in both cases.

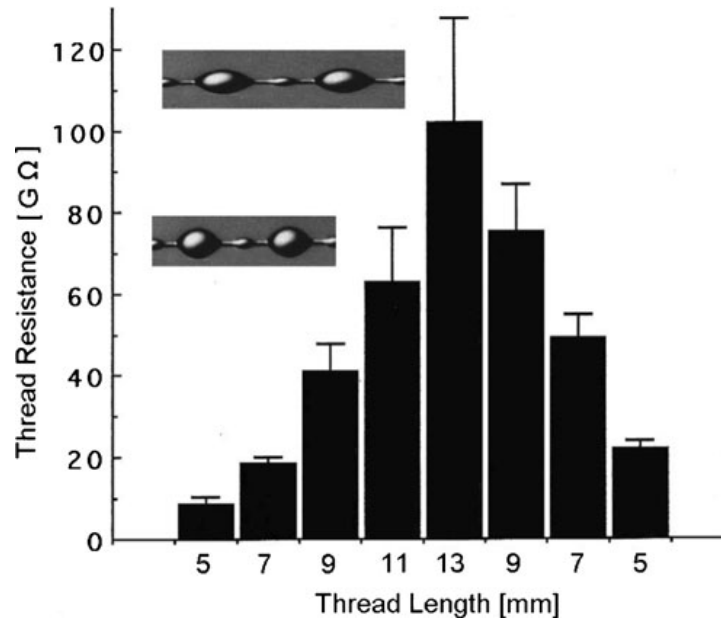


Figure 2.11 Resistance measurements of 5-mm sections of *A. diadematus* web capture spiral as it is being first stretched and then relaxed.

Or measurements of silk conductivity show that the glue droplets are always interconnected by the aqueous coating, which thins but does not break. This of course, is a key to the functional performance of the system that relies on electric charges.

Further studied initiated on these specific silks laid the groundwork for a thorough analysis of the droplet-thread system.

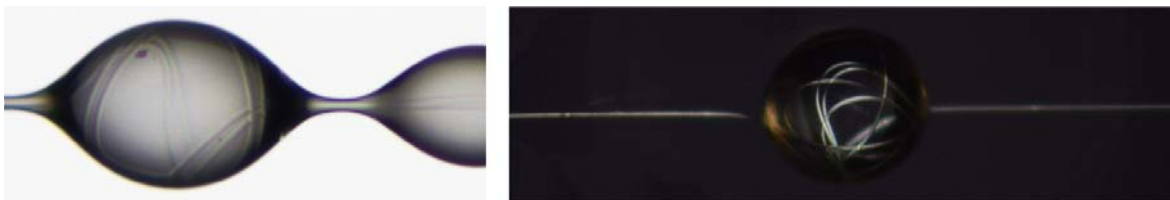


Figure 2.12 Experiments on fibers bent inside liquid drops. Left: microscopic photograph of spider capture silk. Flagelliform core filaments are seen to be coiled and packed inside a (typically 300 μ wide) glue droplet. Right: same mechanism reproduced artificially with a 200 μm synthetic droplet and fiber

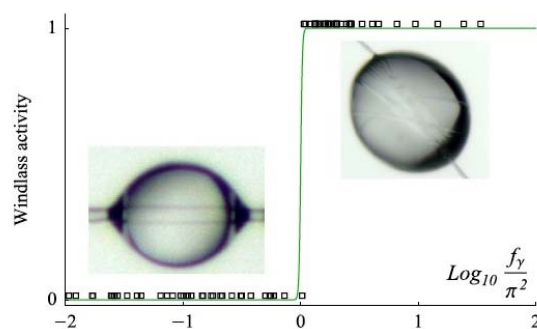


Figure 2.13. Experimental verification of the windlass activation as function of the parameter $f\gamma$. The windlass mechanism is active as soon as the meniscus force $f\gamma$ is, greater than π^2 .

WP (3): Fundamental understanding of Native Composites and Development of Low Temperature Silk Composites.

Natural silkworm cocoons can provide powerful inspiration for synthetic nonwoven composite design. Observing a wide range of different cocoon morphologies and the mechanisms by which they fail under load led us to develop a novel and quantitative design strategy non only for nonwoven composites but also for particulate composites. In that work, it became clear that use of natural silk fibres in conventional fibre reinforced composites offers few advantages in terms of stiffness and strength over conventional composite materials. This led us to investigate the very attractive property combination of strength and toughness of natural silk and its potential advantages over conventional polymers or composites.

Specifically, silks with the right resins can make good to excellent, fully sustainable polymer composites for a wide range of applications. Genercially, natural silk structures provide excellent models for composite design. And can the attractive low temperature properties of natural silk fibres form the basis for a new type of fibre composite material with excellent strength and toughness over a wide range of temperatures and deformation conditions?

Morphological studies of silk worm cocoons

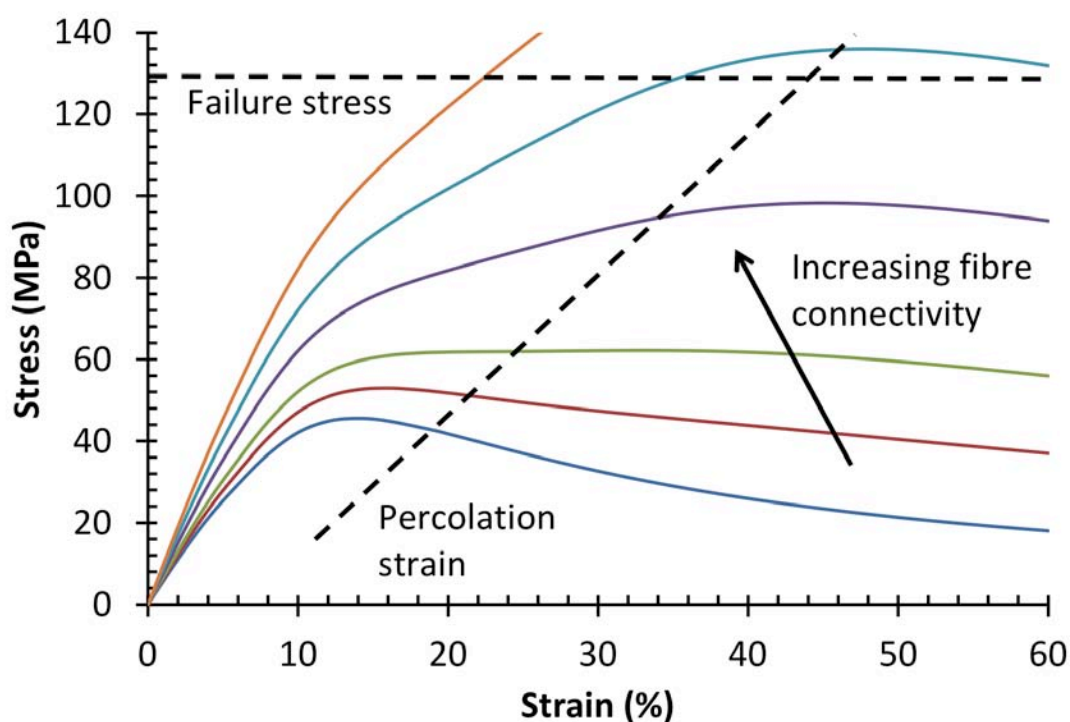


Figure 3.1 A model (based on empirical data on the cocoons shown in Fig3.2 below) for nonwoven cocoons with different amounts of interfibre bonding shows the interrelationships between cocoon strength and sericin binder strength indicated bounded by the dashed line for the percolation strain.

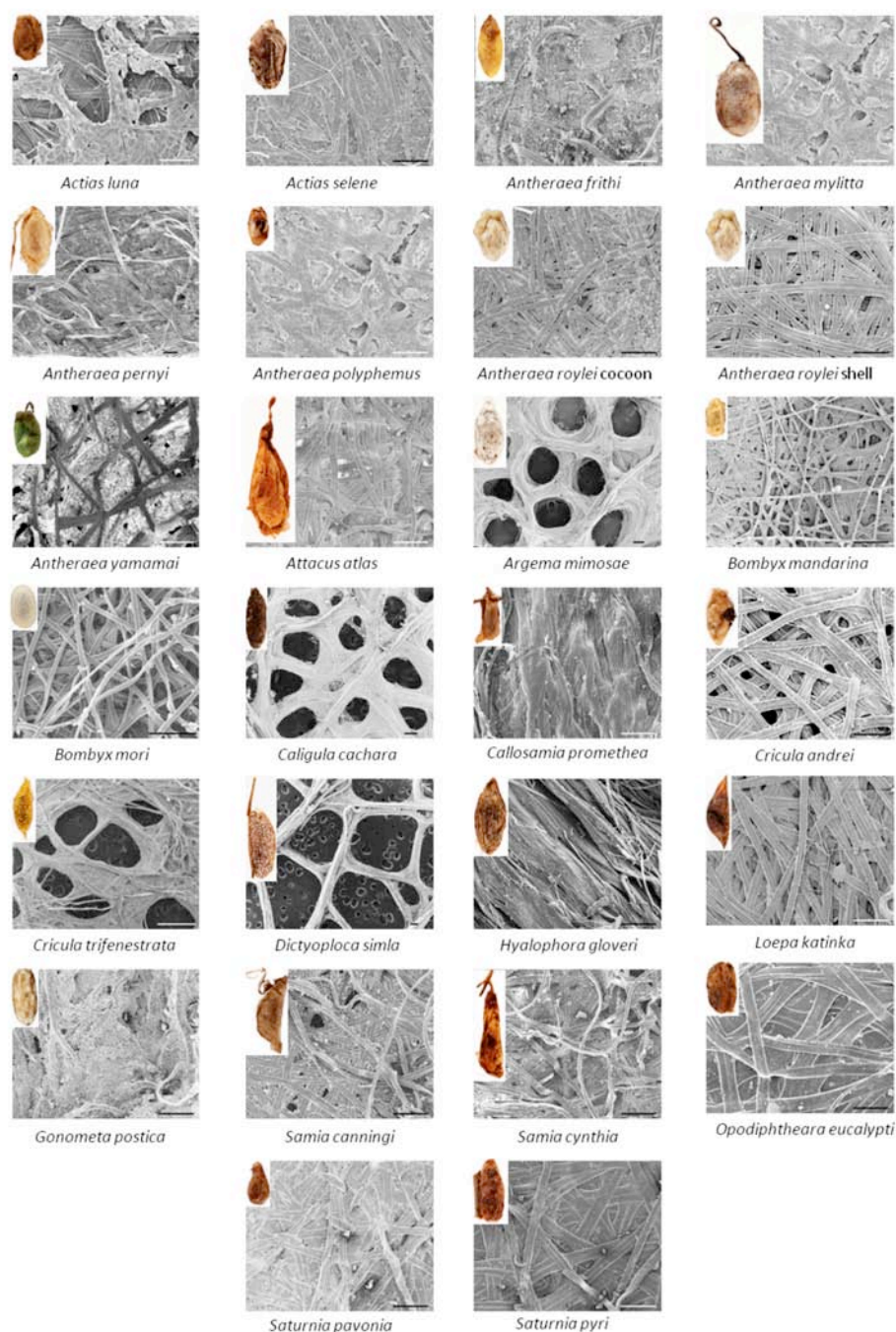


Figure 3.1 Morphology of silkworm cocoons, scale bar: 200µm. Insert: Photos of silkworm cocoons. Every one of the cocoons discussed here has a different combination of morphological features and hence also features different combinations of mechanical and diffusion properties.

To better understand how silkworm cocoons maintain the correct internal moisture levels for successful pupation, we examined cocoons from the long-domesticated mulberry silkworm *Bombyx mori* as well as from two wild, silkworm species, *Antheraea pernyi* and *Philosamia cynthia ricini*. We determined fluid-independent values for the, porosity, tortuosity and permeability of the inner and outer surfaces of cocoons.

Permeabilities were low and, with the exception of *A. pernyi* cocoons, inner surfaces were less permeable than outer surfaces. *B. mori* cocoons, exhibited the highest permeability overall, but only at the outer surface, while *A. pernyi* cocoons appeared to, show different patterns from the other species tested. We discuss our findings in light of the ecophysiology of the various species and propose a 'tortuous path' model to help explain our results. The model describes how the structure of the inner and outer layers of the cocoon allows it to function as both a humidity trap and a waterproof barrier, providing optimum conditions for the successful development of the pupa.

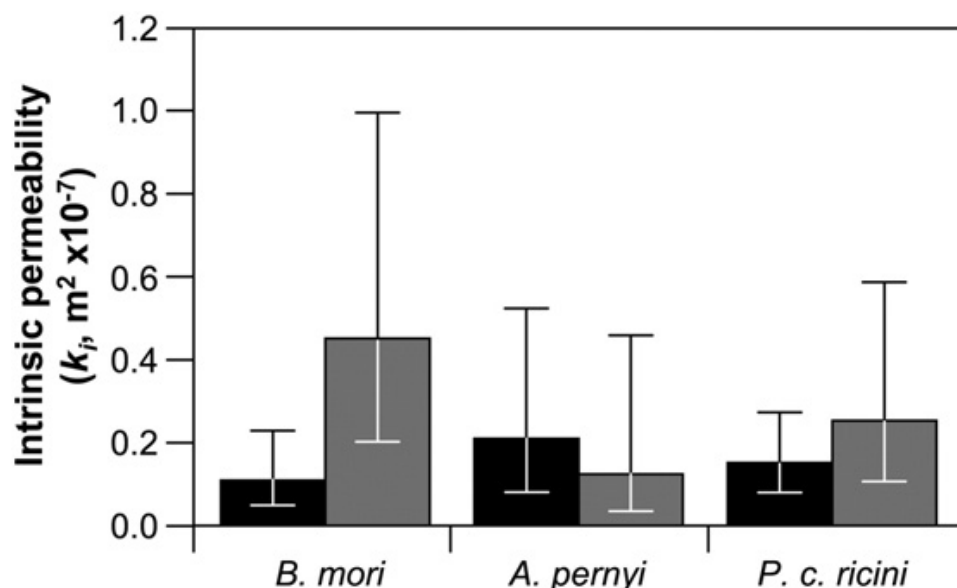


Fig. 3.3 Intrinsic permeability (k_i) values for the inner (black bars) and outer (grey bars) surfaces of cocoon

Silk Diversity

By assessing the diversity of wild silks, we were able to compare native silk feedstock from 6 species and silk cocoons from 35 species using a multivariable analysis approach based on infrared spectroscopy. For unspun native silk feedstocks, we identified spectral markers unique to wild silkworm silks, which we assigned to β -turn secondary structures. This peak could represent an indicator for the feedstock's cell adhesion properties if originating from RGD patterns. To test this hypothesis, the native feedstocks of wild silk species without this pattern would have to be measured. The comparison of the feedstocks also profiled the dissimilarity of Saturniidae silks to the silks of Bombycidae and spiders.

Collecting spectra from silkworm cocoons provided information not only on the spun fiber but also on the non-protein chemical content and distribution of such compounds across the inner and outer layers. Using specific infrared bands, the relative content of sericin, calcium oxalate, phenolic compounds, polyalanine and poly(alanine-glycine) β -sheets was evaluated. Exploiting all the information contained in the infrared spectra, we performed a multivariate analysis on the entire dataset. This analysis permitted the hierarchical classification of 35 species (including one spider silk) into groups based on their chemical composition. This analysis revealed the presence of interesting outlier species with very dissimilar spectra, which could represent distinctive mechanical or chemical properties.

Amongst these outliers were *Gonometa postica* cocoons, which had the highest calcium oxalate of all species measured. Furthermore the species with the most β -sheets, *Epiphora bauhinae*, also appeared to have the closest chemical composition to *Nephila edulis* spider silk dragline. The

Bombyx genus stood out from all other species measured, representing an outlier group. Consequently, using *Bombyx mori* as the model species for silk studies could lead to conclusions that are not applicable to all types of silks. Although our sampling had a bias towards Saturniidae silk, *Antheraea* silks were found to have median principal component scores. This result leads us to speculate that *Antheraea* silks are more representative of silk's biodiversity. Not only did the multivariate analysis classify species of the same genus together, but the ultrametric tree created from the infrared spectra is remarkably close to the phylogenetic tree generated from genetic data. Since this technique also probes the non-protein content, our approach provides information on the silk glands' content, the cocoon's construction behaviour of the animal, as well as the external environment.

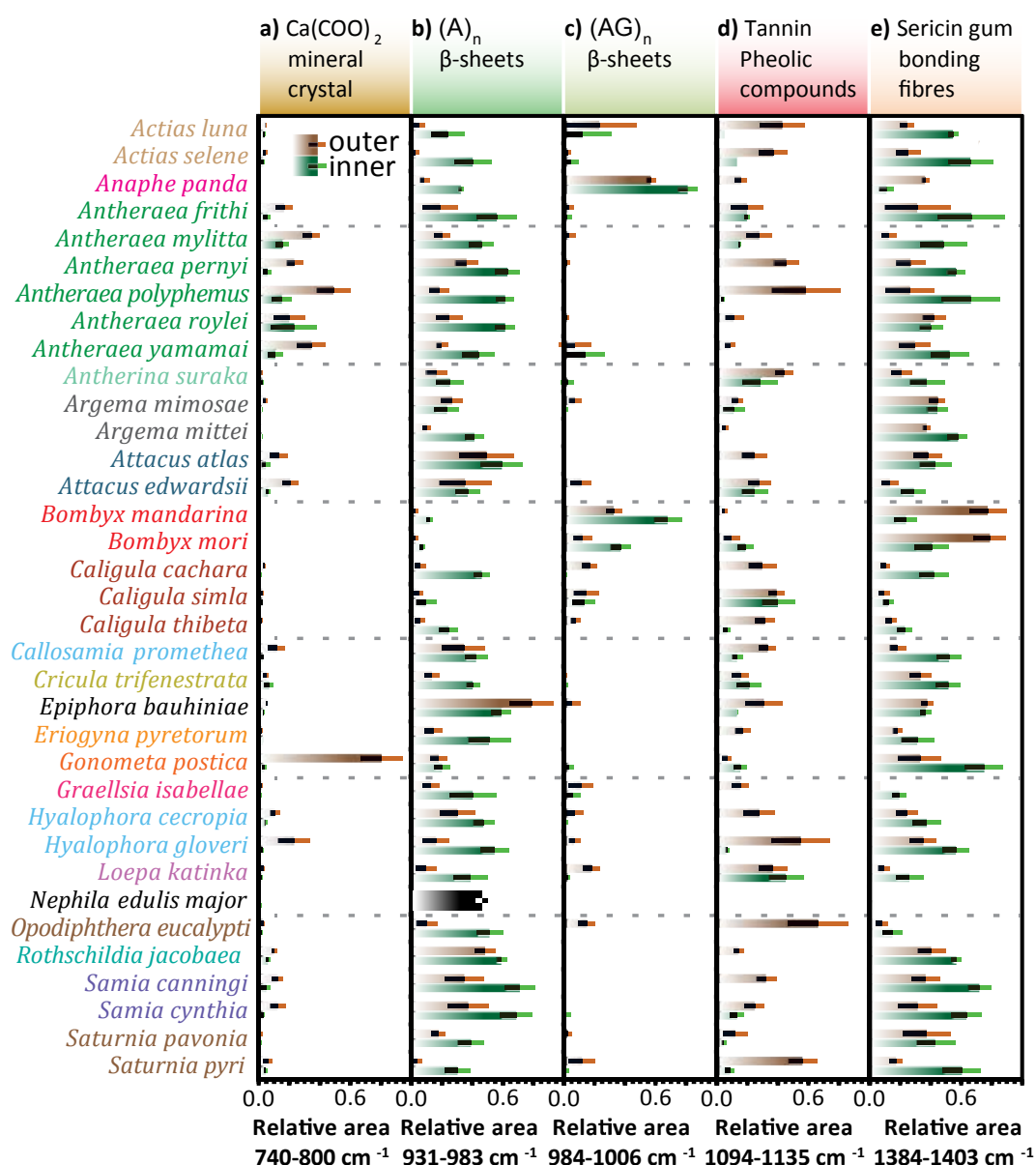


Figure 3.4 a) Relative area of a band assigned to calcium oxalate (740-800 cm^{-1}). b) Relative area of the band associated with $(\text{A})_n$ β -sheets (931-983 cm^{-1}). c) Relative area of a $(\text{AG})_n$ β -sheets assigned band (984-1006 cm^{-1}). d) Relative area of a band associated with tannins (1094-1135 cm^{-1}) d) Relative area of a sericin marker band (1384-1403 cm^{-1}). The outermost layer values are presented by brown bars, and the green bars shows the values of the innermost layer. The error

bars represent the standard deviation of the different observations ($n > 10$). A value of 1 represent the highest area calculated and 0 the minimum measured.

Because of the intense selection pressure on this vital biological structure, we believe silk cocoons represent a model for the phylogenetic analysis including all silk-moths species. This untapped alternative method not only adds to more traditional gene and protein sequencing but is also less time-consuming and cheaper than e.g. protein sequencing. As silk cocoons are commonly part of entomology collections spanning hundreds of years of collecting, they can be readily sourced and rapidly tested in a non-destructive manner providing powerful longitudinal studies into silk-moth evolution and ecology. Furthermore, with the advent of readily affordable handheld IR instruments our approach could also allow such analysis to take place in the field. Thus, ATR-IR combined with a multivariate approach could aid to unravel the evolution and biodiversity of silk producing species as well as inform us regarding which species is best suited to a particular industrial application.

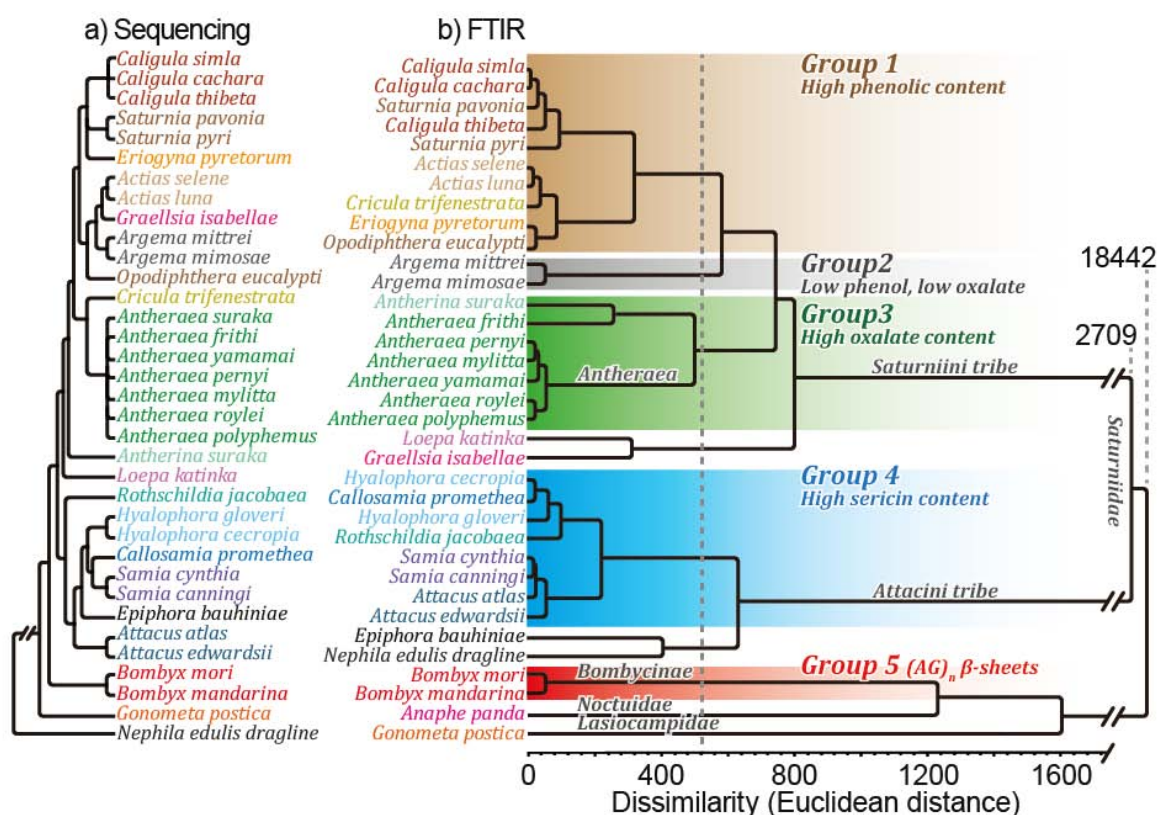


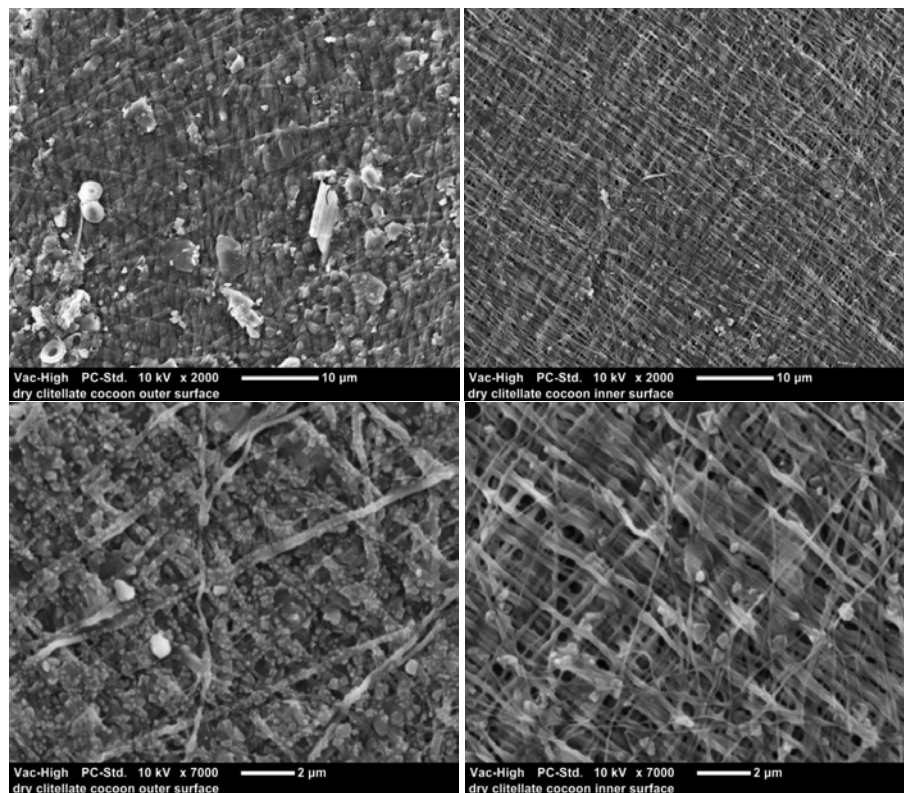
Figure 3.5 a) Cladogram generated from traditional phylogenetic analysis. b) Ultrametric tree generated from the hierarchical clustering analysis of cocoon infrared spectra LDA factor scores. Species with a Euclidean distance smaller than 525 were grouped together.

Morphological studies and mechanical testing of polychaete tubes

In an effort to study a variety of biological structures as model biocomposites, we are interested in biological composite systems that operate in the wet state, unlike the cocoons

which are always dry. In collaboration with Dr Dimitri Deyehn froms SribbsUniversity of California San Diego, we have started to examine the tubes made by the polychaete *Odontosyllis phosphorea*. The worms, which inhabit shallow coastal areas and are benthic (i.e. sea bottom dwellers), build and live inside sac-like tubes made of silk-like material (although the actual material composition has not been studied yet) during the day. The tubes provide shelter to the cryptic worms and possibly allow filtering for food. *O. Phosphorea* have been generally studied for their bioluminescence displays, which the worms use typically for attracting mates, but also possibly for attracting prey and for defence against predation. We focus on the morphology and mechanical properties of the intricate tubes that the worm builds.

To study the morphology of the tubes, we have conducted scanning electron microscopy (SEM) analyses. Hypothesising a potential difference between the morphology of the inner and outer surfaces/layers (from our previous experiences with cocoons of various silkworms), we analysed both the inner and outer surface. Not only did we find the tubes to have enigmatic and impressive netted or felt-like fabric structure, with microfilaments that are bonded to form well-aligned layers, but also find marked differences between the outer and inner surfaces (Fig. 3.).



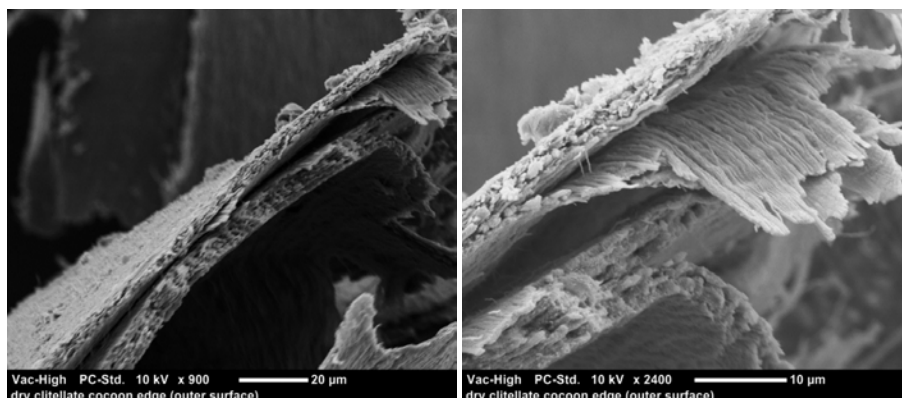


Fig. 3.4. SEM images of worm tubes, showing the a) outer surface (scale bar of 10 µm), b) inner surface (scale bar of 10 µm), c) outer surface (scale bar of 2 µm), d) inner surface (scale bar of 2 µm), e) and f) the unidirectional layered structure of the tubes (scale bars of 20 µm and 10 µm, respectively). Comparing the inner and outer surfaces of the tube, it is observed that the inner surface has less debris/deposits, is less ordered (i.e. there is more fibre 'waviness'), has higher permeability/porosity, and is built of finer microfilaments. It is known that the worm builds the tube from the inside; therefore the outer layer would be built first. However, it is not known whether the difference in structure between the outer and inner layer is there on purpose or a result of the worm tiring and having fewer 'secretions' available – possibly both, *i.e.* the worm utilising its left 'energy' efficiently to provide additional functionality.

A woven structure is not observed; rather it seems that microfilaments are placed on top of one another. The aligned layered structure is clearly visible in

Fig. 3. e) and f). Of particular interest is the fact that the worm produces microfilaments with typical diameters of only 150-350 nm. To produce such a large well-aligned multi-layered tube structure using such thin filaments in a few hours or even minutes would suggest that possibly the worm 'secretes' a large bundle of the microfilaments in a glue-like binding mucus (possibly through glands on its body) and moves periodically in particular directions (e.g. up and down or side-to-side). Essentially, the worm is secreting a mat of semi-glued fibres to produce an aligned structure. Interestingly, this is analogous to the automated tape laying (ATL) technique, which is commonly used in the aerospace industry for the manufacture of composite components for which the fibre orientations are well-defined. In ATL, pre-impregnated tapes of carbon fibre are placed on a surface; the 'tackiness' of the resin ensures that the tape remains stuck to the surface once the robotic head moves ahead (to continue laying the tape).

Apart from studying the intricate morphology of the tube, we also characterised the tensile properties of the tubes (along the longitudinal direction) using a DMTA (in film tension mode and submerged mode) and a universal testing machine. Tests on the DMTA were conducted on both dry samples, and in (seawater) submerged mode. We found that the tensile properties obtained from different instruments were comparable. Dry samples had an average tensile stiffness, strength and elongation of 125 MPa, 0.97 MPa, and 1.14%, respectively, while wet samples (tested in submerged mode and un-submerged mode) had an average tensile stiffness, strength and elongation of 14.1 MPa, 0.91 MPa, 10.7%, respectively. The order of these mechanical properties is similar to rubber-like elastomers. In fact, even spiders produce elastomeric (viscid) silks with a modulus of the order 1 MPa, which have the mechanical properties of a rubberlike polymer.

For reference, stress-strain curves of tubes tested in the DMTA are shown in Fig 3.5. The significantly higher stiffness of the dry samples compared to wet samples is conceivable as the former lack moisture, which swells the structure and the increases the

extensibility/flexibility of the tube. In agreement with this are results from multi-frequency tests on the DMTA which show that as temperature increases from 25 °C to 50 °C, the storage modulus of the tube may increase by 10-30 times. The order of increase in the storage modulus is comparable to the order of difference in the stiffness of the wet and dry samples (14.1 MPa and 125 MPa). It is observed that these tubes then maintain that storage modulus from 50 °C to 125 °C, but in some cases even up to 180 °C. This is indicative of the high thermal resistance of these tubes of marine worms.

TGA analysis of the tubes show that unlike silk fibres and silk fabrics, the thermal degradation profile of tubes from different worms, although shows the same peaks and transitions, is significantly different. Specifically, the residual weight of the tubes (at 800 °C in air) ranges between 30-60%; this compares to a residual weight of silk from silkworm cocoons (at 800 °C in air) of ~2%. This indicates that the tubes have a large and variable content of inorganic/mineral deposits, which is in agreement with the visual observations of the tubes.

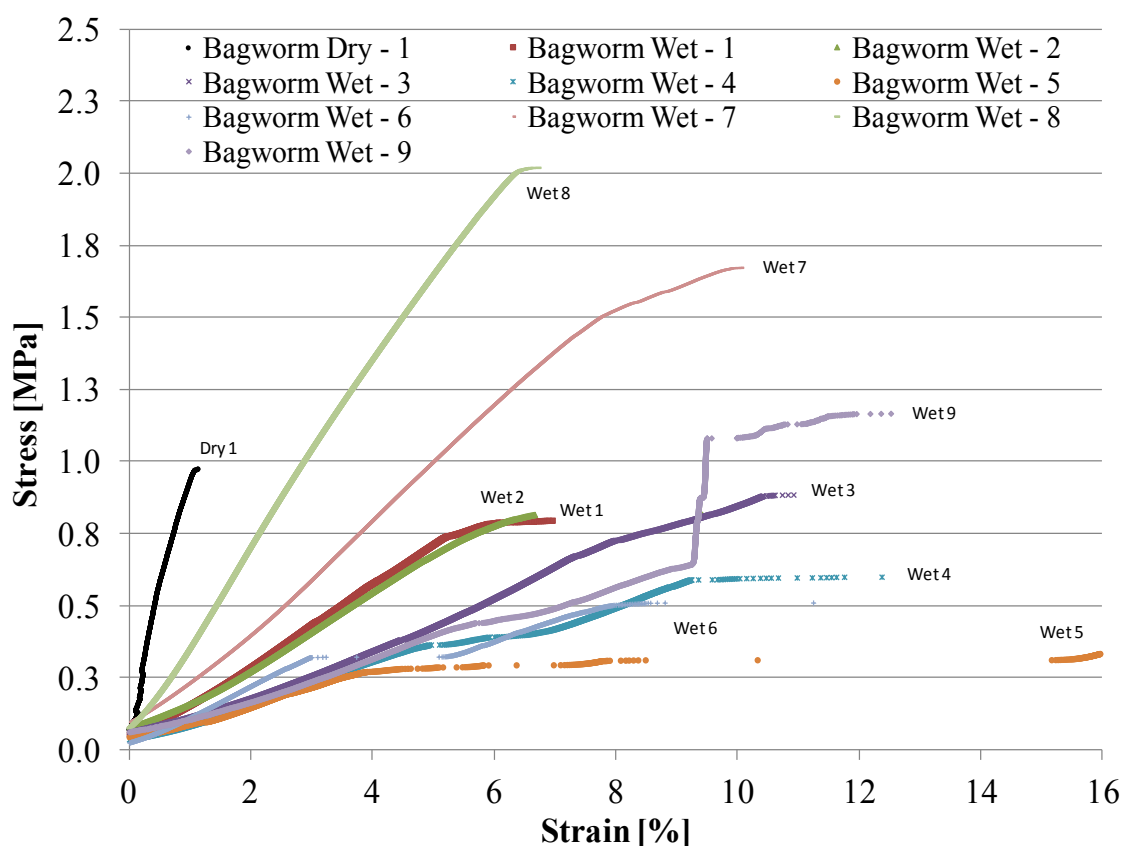


Fig. 3.5 Tensile stress-strain curves of worm tubes tested in the dry state (Dry 1) and wet-and-submerged mode (Wet 1-Wet 8), in a DMTA. Note that specimens were prepared in pairs from the same tube, so Wet 1 and Wet 2 are stress-strain profiles of a specimen from the same tube. It is observed that while there is large variability in mechanical properties between tubes of different worms, there is small variability in mechanical properties of a tube from the same worm.

The ultrastructure and mechanical properties of the tubes were found to comprise of up to twenty multi-axially oriented non-woven plies of aligned nano-scale (\varnothing 50-1,000 nm) fibrils bound together with a diffuse organic matrix. The tubes were consequently referred to as bionanocomposites. Tensile tests on sections of the tube in the wet state elucidated that the mechanical properties of the tube were of the order of viscid silks and synthetic rubber-

like elastomers. Next we conducted i) thorough morphological analyses with a composites manufacture and engineering structure perspective, ii) various mechanical tests, in air and water, under static and dynamic/cyclic loads, and over a wide range of temperatures to evaluate the properties of the tube structure and constituent materials, and iii) time-lapse studies to test our various hypotheses on how the tube is built.

Our recent morphological analyses reveal that the thin-walled, impermeable tubes are bio-inspirational for conventional pipe technology. For instance, we found that the worm uses a venturi tube design with restricted orifices to regulate flow, and facilitate collection of food particles (for feeding) and disposal of waste particles (for tube-cleaning). Interestingly, venturi scrubbers and 'baghouse' fabric filters are widely-used in industry for removing pollutants/contaminants in pipes; both of these are employed by the worm. As a scientific first, we also analysed the orientation distribution of nanofilaments in the different plies of the tubes. This revealed that the dominant orientation angles of nanofilaments in the tube were 0° , $\pm 45^\circ$ and $\pm 65^\circ$. Applying prior knowledge of fibre reinforced polymer composites (FRPs), we found that the dominant orientation angles correlated well with optimal winding angles for FRP pipes and vessels subjected to specific loading conditions. 0° plies are ideal for bending and axial loads, $\pm 45^\circ$ plies are optimal for torsion/shear loads, and $\pm 65^\circ$ plies are suitable for combined external pressure and buckling loads. Consequently, we hypothesised that the biocomposite tube structures have evolved to confer a high degree of mechanical stability and resistance against deformation and tearing forces.

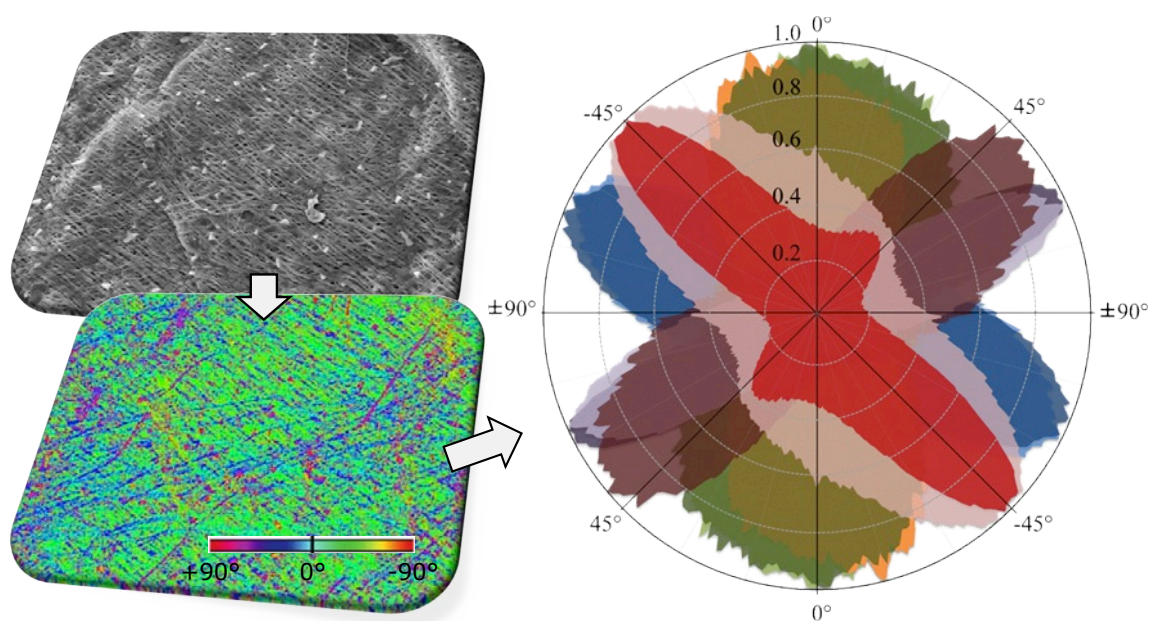


Figure 3.6 Image analysis of Chaetopterus tube surfaces to determine the distribution of orientation of nanofilaments in a layer, and variation in orientation between layers and tubes. For example, a tube surface and a processed colour-coded image of the surface are shown. Superimposed circular intensity histograms of ten typical tube surfaces (different colours) are also shown. By convention, 0° is along the length of the tube, while $\pm 90^\circ$ is transverse to the tube length. On each surface, nanofilaments were principally oriented in one direction only, with no preferred second-best orientation. The principal or dominant orientation angles were 0° , $\pm 45^\circ$ and $\pm 65^\circ$.

As part of testing the above-mentioned hypotheses, we conducted a thorough characterisation study. The tube material exhibited thermal and thermo-oxidative stability up to 250°C , similar to other biological materials like mulberry silkworm cocoons. Unlike silks, which have characteristic amorphous phases and exhibit a glass transition temperature (of $\sim 200^\circ\text{C}$), dynamic mechanical thermal analysis conducted in both air and water elucidated the lack of a glass transition in the organic tube wall material (Figure 1). In fact,

the visco-elastic properties of the anhydrous and undried tube were remarkably stable (i.e. constant and reversible) between -75 and 200 °C in air and 5 and 75 °C in water, respectively. These observations indicated that the organic material ought to be highly crystalline or cross-linked, and strongly bonded (through covalent or extensive hydrogen bonds) at an intra-molecular level. However, if the tube were to consist of highly networked components, the elastic modulus of the dry tube structure would be higher than that is observed: of the order of $2\text{--}3$ GPa rather than the observed $0.3\text{--}0.5$ GPa. Structural features including porosity, complex fibre sub-structure (e.g. hollow nanofibrils) and the multi-axial ('mis-')orientation of the anisotropic nanofibrils are the suggested likely sources of the low elastic modulus of the tube material.

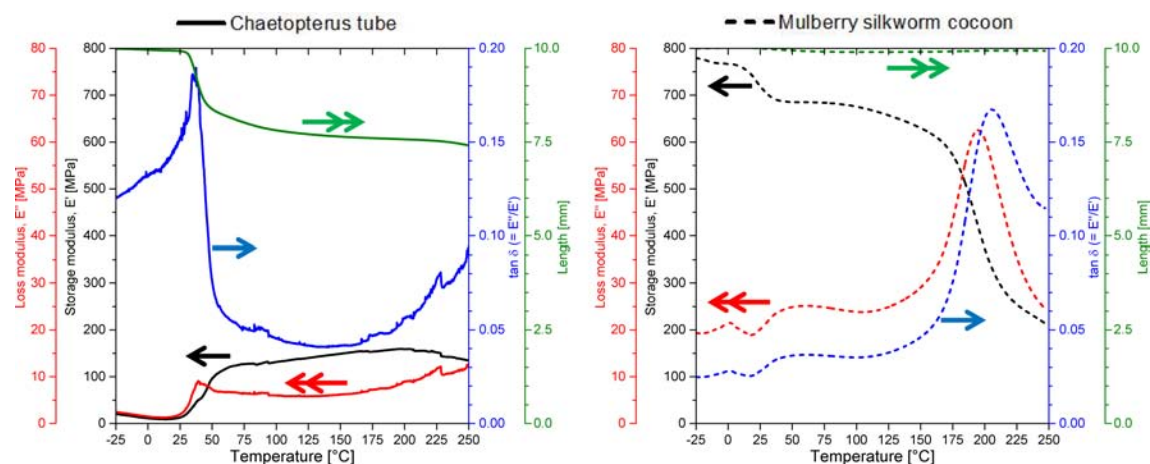


Figure 1.7 Comparison of visco-elastic property profile of Chaetopterus tubes and mulberry silkworm cocoons tested in air over a temperature range of -25 to 250 °C. Note the presence of a glass transition in the cocoon but not in the tube. In the temperature range studied, the tubes became more glass-like (less damping) with increasing temperature, while silkworm cocoons become more rubber-like (more damping).

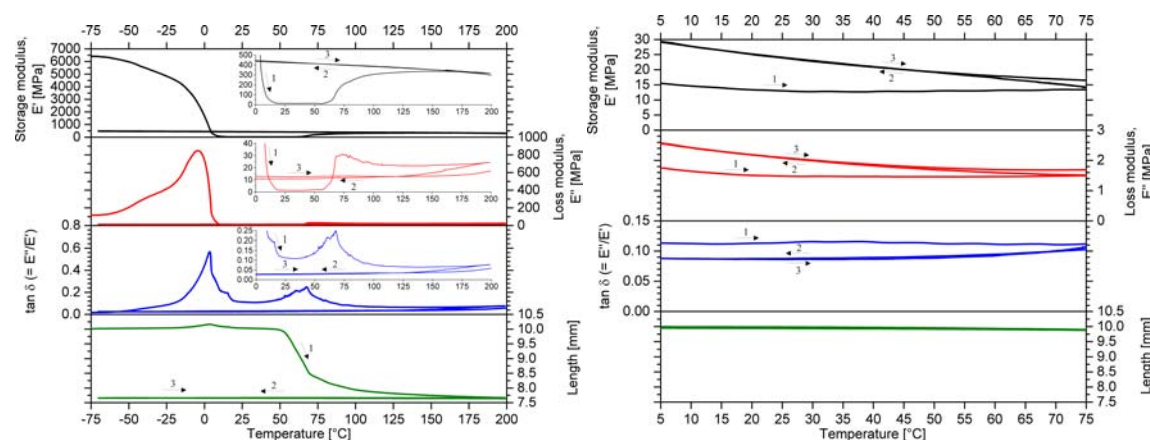


Figure 3.8 Thermal cycling of the tubes between -75 and 200 °C in air (left) and between 5 and 75 °C in water submersion mode (right) revealed that hydration and associated-water plasticization were key to its rubber-like properties. Moreover, both the dried and undried tube had remarkably stable and reversible properties across the entire temperature range.

Mechanical property characterisation in the longitudinal and transverse directions ascertained that the tubes were not quasi-isotropic structures. In general, the higher stiffness and strength in the transverse direction implied that there were more nanofibrils oriented at $\pm 45^\circ$ and $\pm 65^\circ$ than at 0° to the tube axis. Notably, the complex orientation of the filaments had a governing effect on the mixed-mode fracture mechanism.

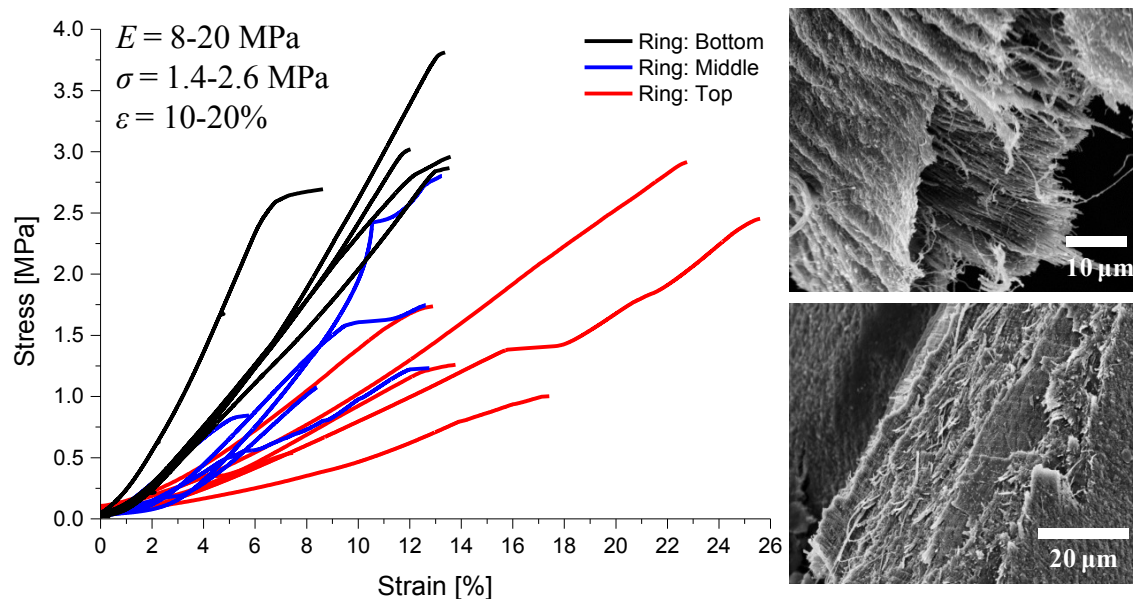


Figure 2.9 Evolution for function: the stress-strain behaviour changes along the tube length. It is notable that such a transition in stress-strain profiles and properties is observed in FRPs when fibre orientation is changed. The high failure strain or toughness of the tubes was a result of distributed deformation, feasible from i) the complex orientation of the fibrils, ii) stress-transfer and strain-accumulation at the large surface area fibre-matrix interface, and iii) non-woven laminate structure.

Not only are the tube structure and material unusual, but so is the tube production mechanism. Our time-lapse studies show that, contrary to generic assumptions in literature, the worm actively, rapidly and sporadically produces and expands the tube. Indeed, the fine organisation of the nanofilaments observed in the tubes strengthens the case for ‘active’ rather than ‘passive’ tube building. The presence of numerous folds and wrinkles on the surface, which have been described to be the edges of individual layers, also suggest sporadic growth. We hypothesize that the very first layer is a template that coordinates all the successive layers. Our very recent studies on the effects of temperature on tube building indicate that the self-organization of the tube is not driven by the worm, but by the chemical reaction (possibly branching, cross-linking i.e. polymerization) of the mucus.

Our collaboration with Dr DD Deheyn is continuing with the aim to i) examine the chemical composition and possibly fine microstructural details (e.g. cross-section of nanofilaments, and transmission electron microscopy) of the tube wall material, and ii) further examine the tube production mechanism. The studies are of interest to the biomaterials research community (and possible model materials) noting that such complex-oriented bionanocomposite tubes with exceptionally broad thermomechanical properties are produced rapidly by the worm underwater, using possibly the same mucous that the worm also employs to i) filter food (via a mucous bag), and ii) attract mates/prey or for defence against predation using bioluminescence.

Investigating natural rubber (latex)

As a possible matrix/resin material for our silk-based composites we have inter alia investigated natural latex, not least as it is currently used in top-quality silk-based racing cycle tyres. Natural latex is a material of significant scientific and commercial interest. Latex is most likely used by laticifer plants in defence against herbivory deploying two separate defensive mechanisms: biochemical and mechanical. Natural rubber (cis-1,4-polyisoprene) is

found in high concentrations in many latex, and finds many applications in industry. A collaborating with the Kasetsart Agricultural and Agro-Industrial Product Improvement Institute (Kasetsart University, Thailand) is ongoing with the aim to develop silk reinforced natural rubber composites.

When studying the *Chaetopterus* biocomposite tubes, we were employing a materials science approach to gain insights in a materials science framework (e.g. tube structure and constituent materials, and tube production process). Here, we were interested in studying plant latex through a materials science perspective to allow interpretations in an biological, evolutionary framework. Specifically, we wanted to probe the rheological properties (i.e. shear deformation and flow properties) of latex to determine it's biological function and the evolutionary pathway to its development.

We performed detailed quantitative studies on the flow characteristics of microlitre samples of native latex from two plant genera, *Euphorbia* and *Ficus*. From a rheological perspective, latex behaves like a complex colloidal suspension of a polymeric substance in an aqueous medium. Our findings reveal that in laboratory conditions both latices behave like non-Newtonian materials with the coagulation (increase in viscosity and modulus) of *Euphorbia* latex being mediated by a slow evaporative process (more than 60 min), whereas *Ficus* appears to use additional biochemical components to increase the rate of coagulation (more than 30 min). Slow drying and coagulation times are ideal if predators are to be exposed to anti-herbivory compounds for as long as possible. On the other hand, for wound healing, a rapid increase in mechanical properties over the shortest period of time is ideal. Based on these results, we propose two different primary defensive roles for latex in these plants: the delivery of anti-herbivory compounds (*Euphorbia*) and rapid wound healing (*Ficus*).

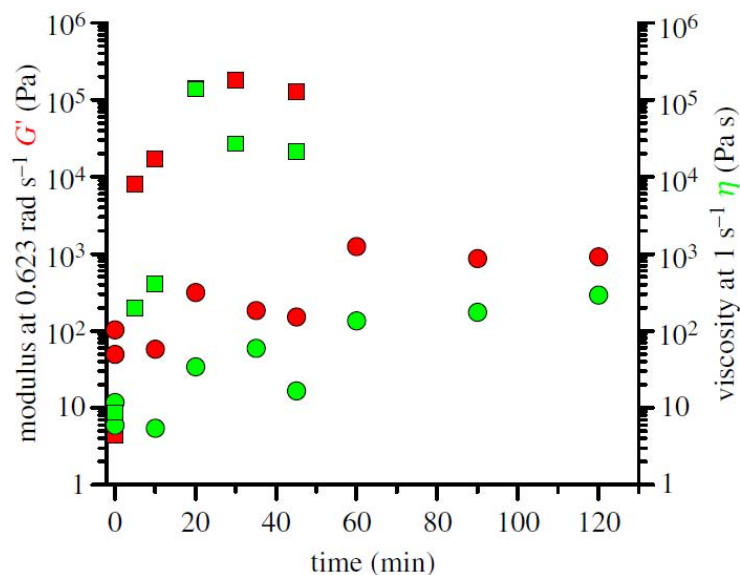


Figure 3.10 Property-time plot of exuded latex of *Euphorbia* (circles) and *Ficus* (squares) (elastic modulus at 0.623 rad s⁻¹ (0.1 Hz), red; viscosity at 1 s⁻¹, green). Datapoints represent individual samples from each species.

In the future, we envisage the application of microrheological techniques to continue to help elucidate the true nature of these multi-functional materials, leading us forward in both fundamental understanding and industrial applications. We will also specifically investigate the rheological properties of purified natural rubber and whole natural rubber to

appreciate the effects of processing (and the presence/absence of natural impurities) on the rheological properties.

Design and development of silk-reinforced composites

From our thorough characterisation studies on natural silkworm cocoons and fibres extracted from such cocoons, we had previously concluded that natural silk fibres and cocoons are powerful inspirations for the design and modelling of i) synthetic fibres and polymers producible through ultra-low energy processing routes, and ii) synthetic nonwoven and particulate composites. Moreover, we had previously identified nature's wonder-fibre silk as a strong natural fibre candidate for reinforcements in polymer composites (Table 1).

Table 1. Silks offer various advantages over plant and glass fibres in reinforcing composites, particular low density, high compliance and high toughness.

Properties	Silk fibres ^a		Plant fibres ^b		Glass fibres ^c
Annual global production of fibres [kt]	(150)		31,000	(600)	4,000
Cost of commercial raw fibre [£/kg]	(2.0-30.0)		0.5-1.5		1.3-20.0
Chemical nature	protein-based		cellulose-based		silica-based
Fibre length	continuous		discrete		continuous
Fibre diameter [µm]	1-15	(8-15)	15-600	(15-50)	5-25
Density [gcm ⁻³]	1.25-1.35		1.35-1.55		2.40-2.70
Moisture absorption [%]	5-35	(20-35)	7-25	(7-10)	0-1
Softening temperature [°C]	170-220		190-230		700-1,100
Tensile stiffness [GPa]	5-25	(5-15)	30-80	(50-80)	70-85
Specific tensile stiffness [GPa/gcm ⁻³]	4-20	(4-12)	20-60	(30-60)	27-34
Tensile strength [GPa]	0.2-1.8	(0.3-0.6)	0.4-1.5	(0.5-0.9)	2.0-3.7
Specific tensile strength [GPa/gcm ⁻³]	0.1-1.5	(0.3-0.7)	0.3-1.1	(0.3-0.7)	0.7-1.5
Tensile failure strain [%]	15-60	(15-25)	2-30	(2-4)	2.5-5.3
Toughness [MJm ⁻³]	25-250	(70)	5-35	(7-14)	40-50
Specific toughness [MJm ⁻³ /gcm ⁻³]	20-185	(50-55)	3-26	(4-10)	16-19

^a Includes silks from various spiders and silkworms. As most of the commercial silk is cultivated from the *Bombyx mori* silkworm, typical properties of this variety of silk are presented in brackets.

^b Includes bast, leaf and seed fibres. Typical properties of flax fibre are presented in brackets.

^c Includes E- and S-glass fibres. Properties for E-glass are in the lower range.

To systemically investigate the potential of silks as effective reinforcements, we have now examined their reinforcing ability in both fibre reinforced composites [i.e. textile composites] and particulate composites [i.e. cocoons as hollow macrosphere particulates in bio-foams]. The results obtained so far are described in the subsequent sections.

Silk textile composites

In developing silk textile composites with useful properties, the first hurdle we tackled was on the 'design and manufacture' of silk fibre composites (SFRPs). To aid this, over the last year, we conducted an extensive, critical literature review, and simultaneously

worked on the fundamental design philosophy of composites noting the apparent differences between the traditionally used brittle-stiff reinforcing fibres (such as flax, glass, carbon) and ductile-compliant silk fibres. Based on these, we highlighted three key recommendations in the development of SFRPs. Firstly, the comparable stiffness of silk fibres to commonly used matrices ($E_f/E_m = 1-5$ for silk-epoxy) implies that fibre volume fractions v_f in, for instance unidirectional SFRPs need to be i) $>20-40\%$ to ensure that fibres carry at least equal load as the matrix (i.e. $P_f/P_m \geq 1$), and ii) $>60\%$ to ensure that fibres carry at least ten times more load than the matrix (i.e. $P_f/P_m \geq 10$). The required fibre volume fractions are much lower for traditional reinforcing fibres due to their higher stiffness. It is telling that most studies in literature on SFRPs have targeted fibre volume fractions of $<30\%$, leading to composites with properties similar to that of the neat matrix. Secondly, for compatibility (viz. property and processing) with the silk fibre, a thermosetting matrix with high-failure strain, low-processing temperature, and low viscosity needs to be selected. In particular, liquid composite moulding processes such as vacuum-driven resin transfer moulding (VARTM), are more suitable for silk (and other natural fibres) than injection or compression moulding processes. Thirdly, given the lack of studies investigating fracture energy dissipation mechanisms in SFRPs, we proposed that long ($>> 4\text{mm}$) silk fibres that were not actively surface treated may provide adequate fibre/matrix adhesion. The latter suggestion particularly acknowledged that interface modification was avoided due to its complex, sometimes detrimental, effects on toughness.

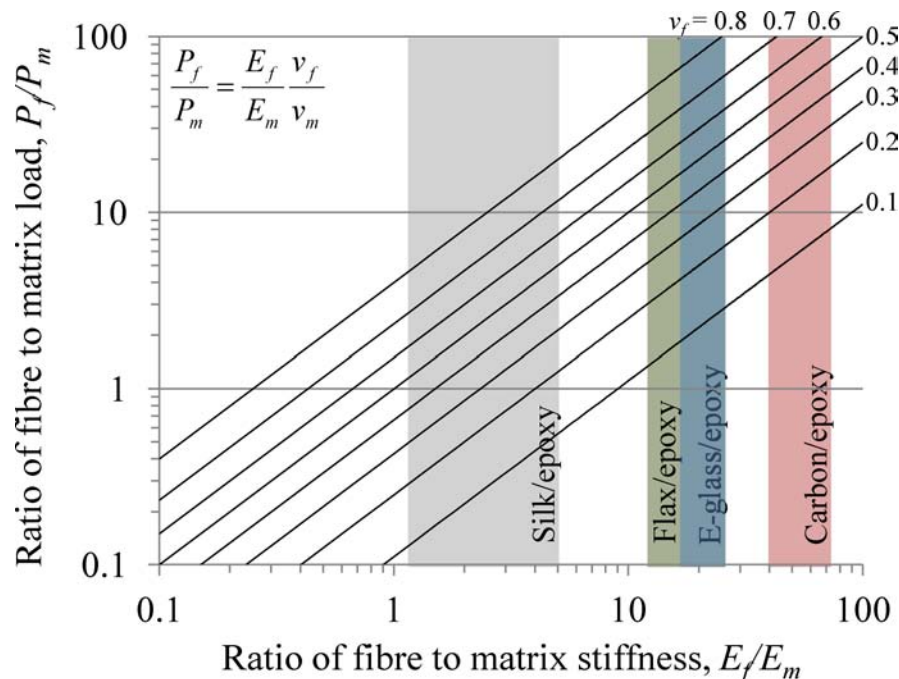


Figure 3.11 The ratio of the load carried by unidirectional fibres to the load carried by the diffuse matrix, P_f/P_m is proportional to the ratio of the elastic moduli, E_f/E_m and the volumetric ratio, v_f/v_m . For maximum reinforcement (i.e. fibre taking most of the load), E_f/E_m and v_f/v_m should be maximised. Due to the low stiffness of silk, its combination with traditional matrices (such as epoxy) results in low E_f/E_m ratios (1-5 for silk-epoxy). Stiff fibres such as flax, E-glass and carbon, impart higher E_f/E_m ratios (12-25, 17-25 and 40-75 for flax-epoxy, E-glass-epoxy and carbon-epoxy, respectively). Consequently, while unidirectional flax and E-glass fibres would carry at least 10 times the load carried by an epoxy matrix at fibre volume fractions above 30% (i.e. $P_f/P_m \geq 10$ for $v_f > 0.3$), unidirectional silk fibres would carry at least 10 times the load carried by an epoxy matrix at fibre volume fractions only above 60% (i.e. $P_f/P_m \geq 10$ for $v_f > 0.6$).

Consequent to these findings, we identified suitable commercially-available, high-toughness, compatible resin systems (most notably, Momentive RIM R135 + RIM H137 epoxy system) for our silk fibres. In the previous year's AFOSR report, we had presented initial

mechanical characterisation data on silk composites (at 30% fibre volume fraction) manufactured using a hand-layup technique. Over this 2nd year, we produced an all-aluminium resin transfer moulding (RTM) tool to produce high-quality composites.

To better understand and optimise the critical mould filling stage in the liquid moulding process, we carried out fundamental studies on the through-thickness compaction behaviour of silk textile preforms. The compaction behaviour of technical textiles affects the reinforcement permeability and part fill time in the mould filling process, and also determines the thickness and volumetric composition (i.e. fibre volume fraction) of the final part. While it is common knowledge in natural fibre composites manufacture that plant fibre reinforcements are considerably less compactable than synthetic fibre reinforcements, the through-thickness compaction behaviour of animal-fibre silk reinforcements has not been characterised thus far. Our important studies revealed that not only are silk reinforcements significantly more compressible than plant fibre reinforcements, but their compactability exceeds that of even glass fibre textiles. For instance, the fibre volume fraction (at a compaction pressure of 2.0 bar) of woven biaxial fabrics of silk, plant fibres and E-glass are 54-57%, 30-40% and 49-54%, respectively. Therefore, silks provide an opportunity to manufacture high fibre content natural fibre composites; this is a bottleneck of plant fibre textiles.

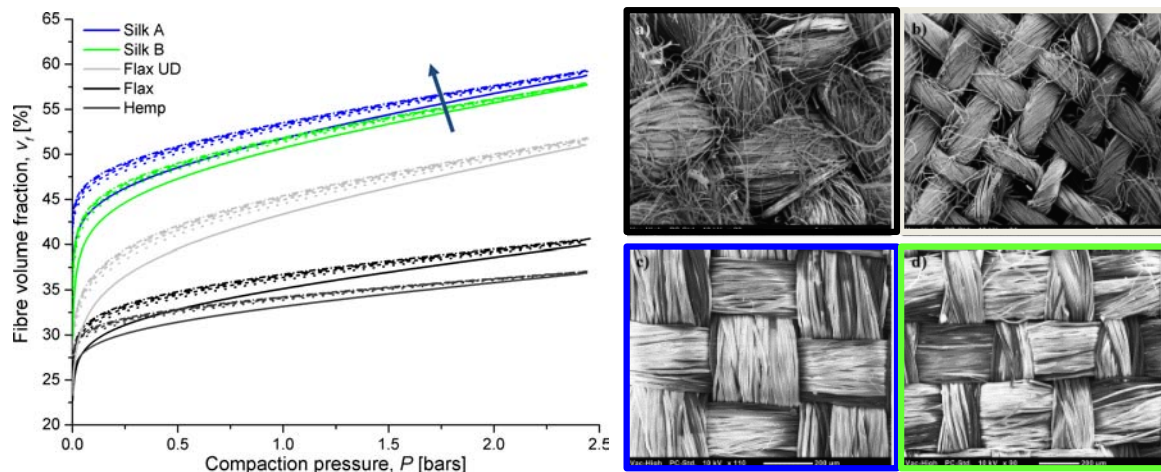


Figure 3.12 Silk textiles are more significantly compactable than plant fibre and glass fibre textiles. Comparing the structure of silk and plant fibre textiles through scanning electron microscopy, we showed that favourable fibre/yarn/fabric geometry, high degree of fibre alignment and dispersion, and suitable technical fibre properties enable optimal packing and arrangement of silk textiles.

Our progress in understanding the critical design considerations for SFRPs enabled us to manufacture high-fibre volume fraction nonwoven (i.e. nominally 2D randomly-oriented fibre) and plain-woven silk composites. The in-house produced nonwoven silk mat reinforcement is unique as our low-cost, patented, steam-pressing fabrication process preserves the continuous length of the silk fibres by relying on the melt flow of the already present natural binder (namely, sericin) in the cocoons to binds adjacent shells. Composites with fibre volume fractions in the range of 35 to 45% were produced, with void content of less than 5%.

To evaluate their potential and determine appropriate applications, the silk composites were then compared to similar flax and glass fibre reinforced composites. Such a comprehensive cross-comparative study on sustainable composites is not found in literature so far. While the fibre content of the flax and glass composites were in a similar range to the silk composites, the composite densities were in the following order: silk \leq flax < glass. We

measured the tensile, flexural, interlaminar shear, and impact toughness properties of the composites.



Figure 3.12 Silk composite laminates: Nonwoven mat (left) and biaxial woven fabric (right) reinforcements.

The tensile and flexural moduli of the *i)* nonwoven and *ii)* plain woven silk composites were in the range of *i)* 5.2-5.4 GPa, and *ii)* 6.4-6.5 GPa. The tensile strength of nonwoven and woven silk composites was 60 ± 5 MPa and 111 ± 2 MPa, respectively. The flexural strengths were 2.3-2.4 times higher than the tensile strengths. Clearly, in terms of absolute flexural properties, silk composites lie comfortably between glass and flax composites (and expectedly, woven composites lie above nonwoven composites). Notably, the woven silk composite demonstrated high fracture strain capacities, which may be particularly attractive in applications where progressive failure or high compliance is required. This is unlike the relatively brittle nature of flax and glass fibres and their composites.

Proteinaceous silk fibres have a lower density than both lignocellulosic flax fibres and inorganic glass fibres. The resulting composites also showed a similar trend. As reducing weight is a top priority in many applications, natural silk composites offer an enhanced opportunity (with respect to plant fibre composites). In addition, considering the specific properties becomes of interest. presents flexural stress-strain curves normalised for the material density. We found that while the stress-strain profiles of silk, flax and glass composites lay almost super-imposed, silk composites were relatively superior to both flax and glass composites in terms of specific flexural properties, particularly noting the high failure strain of woven silk composites.

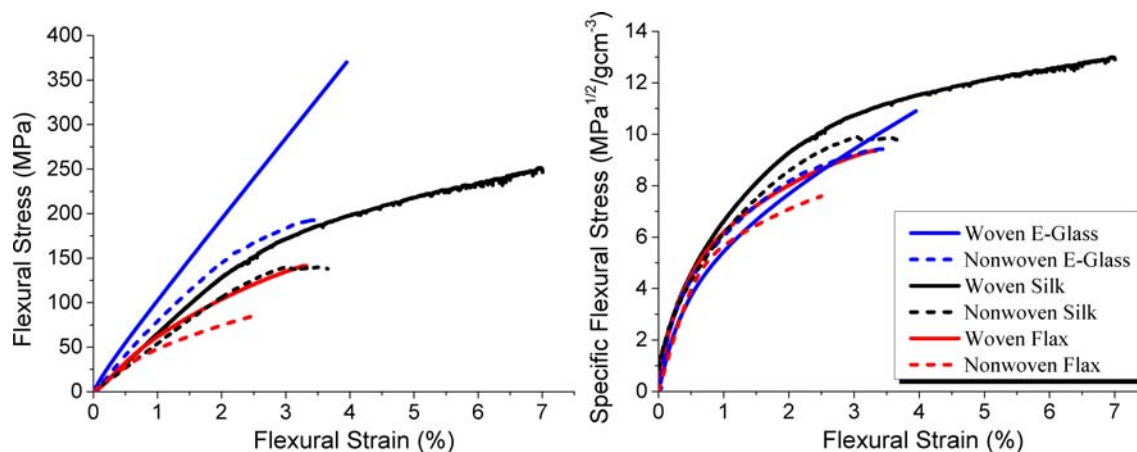


Figure 3.13 Typical stress-strain profiles comparing flexural and specific flexural properties of nonwoven and woven silk, flax and E-glass composites.

We found that the absolute and specific tensile properties of silk composites compared well to flax composites, but were significantly lower than that of glass composites. Silk composites performed significantly better in flexural mode.

Poor impact strength and low interfacial strength have often been described as the principal Achilles heels of plant fibre composites. We found that silk composites outperformed flax composites in those departments, and were more comparable to, but not better than, glass fibre composites. Nonwoven silk composites had an ILSS of 31.0 ± 3.7 MPa, while woven silk composites had an ILSS of 42.6 ± 5.9 MPa. Estimates of the critical fibre length are at 0.2-0.4 mm. The high interfacial bonding between the silk fibres and the polar epoxy matrix achieved without any active surface modification was revealing as a similar interfacial bonding for glass composites is only obtained due to the silane-based surface treatment of composite-grade glass fibres. The high impact strength of the woven silk composites (115 kJm^{-2}), on the other hand, was not surprising given the enviable balance of strength and ductility of silk fibres, and the high failure strain capacities of their composites.

We found that silk composites are an excellent alternative to plant fibre composites, and even a potential sustainable option against glass composites, in appropriate applications; for instance, in i) light-weight, tough components, such as high-performance helmets and aerial surveying drones, and ii) light-weight, flexural stiffness- or strength-critical components, such as composite construction beams, automotive load floors, and sporting equipment. As a demonstrator part, we have manufactured a silk textile reinforced composite shell ($v_f = 30\%$) of a crash helmet. Certainly, depending on the application, other factors such as materials cost and materials environmental aging properties will require attention. Indeed, over the last year we have carried out life cycle assessment of silk fibre, by analysing energy demands in mulberry production, silkworm rearing, and silk processing (discussed in a later section). In the coming year, we aim to use this data to extend our life cycle studies into the sustainability of silk reinforced polymer composites.

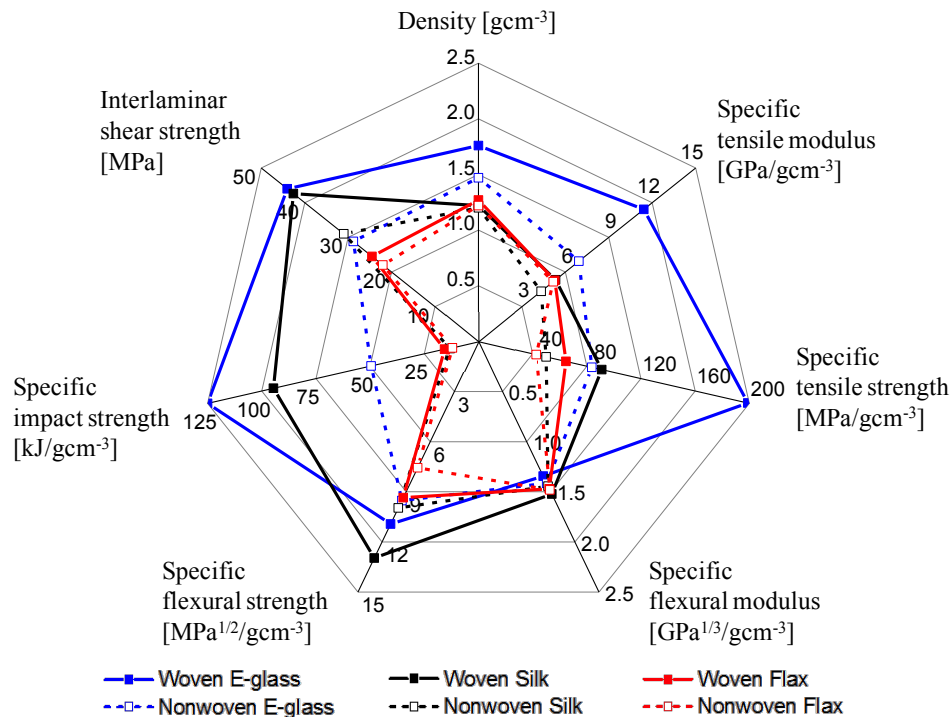


Figure 3.14 Comparison of various mechanical properties of nonwoven and woven silk, flax and E-glass composites.

From our work so far, it is evident that silks make a strong case for polymer reinforcing fibres, particularly as superior alternatives to other natural fibres. In the coming year, we aim to primarily focus on i) 'green composite' development – where silk fibres are reinforcements for bio-based, if not natural thermoset resin systems (rather than synthetic, petro-chemical derived resin systems), and ii) fundamental studies on the fibre/matrix interface characterisation. For the first part of the study, we have already acquired two suitable sustainable resins (namely, 100% natural Furan bioresin derived from plant hemicellulose, and a cashew nut seed oil based (30-40% bio-content) polyurethane). We will be preparing the silk reinforced composites in the next coming weeks and characterising their mechanical properties, in comparison to silk composites with synthetic matrices. For interfacial studies, we are collaborating with Dr JW Gilman's group (National Institute of Standards and Technology, USA). We will evaluate the fibre matrix interface at several scales: nano-level, micro-level, and macro-level. For nano-level testing, we will be trialing Förster resonance energy transfer (FRET) technique, and more excitingly, the use of UV-light/strain/stress-activated mechanophores that polymerise with the resin matrix and adhere to the reinforcing fibre, to provide a molecular-scale reading of the local mechanical state at the interface. The results will be compared to micro-level tests (e.g. micro-bond tests, pull-out tests, and single fibre fragmentation tests) and macro-level tests (e.g. short beam shear tests, 15° off-axis tensile tests or $\pm 45^\circ$ tensile tests). We have already conducted preliminary studies on micro-scale interface testing through pull-out tests on silk/hydrogel composites, and macro-scale interface testing through short-beam shear tests on silk textile composites. The mechanophore-based techniques we look to co-develop will not only improve our understanding of silk reinforced polymer composites, but enable studying the interface of all polymer composites, particularly ductile fibre-brittle matrix systems.

Silk cocoon reinforced biofoams

While silk fibres are engineering fibres with impressive properties, the cocoons of silkworm caterpillars, from which we unravel silk filaments, are themselves remarkable engineering composite structures. The cocoons have evolved over millions of years to protect the larvae from predators during the vulnerable phase of worm-to-moth transformation. They are built by the animals using a continuous dual-strand of silk fibroin (1000-1500 m in length) coated with ~15-30 wt% sericin binder. While silk fibroin is a hydrophobic fibrous protein polymer with a semi-crystalline structure, sericin is a highly-hydrophilic amorphous protein polymer. Some species, such as the wild African silkworm *Gonometa postica*, are also known to include a fraction (<5 wt%) of particulate minerals, namely calcium oxalate crystals, to reinforce the external cocoon structure. Broadly speaking, silkworm cocoon shells have a non-woven polymer composite laminate structure. We have previously evaluated the impact resistance and damage tolerance of cocoon shells, and have developed stochastic models based on open-cell foam structures to study natural silkworm cocoon shells as model materials for the failure analysis of synthetic non-woven composites.

With the growing interest in material technologies incorporating bio-based constituents, several researchers have investigated substitutes to both conventional polymer foams and their synthetic reinforcements for syntactic foams. As eco-friendly filler materials, i) powdered nano-fillers from renewable sources such as clay and chitin, ii) microcrystalline cellulose and wood flour, and iii) short (0.1–5 mm long) and long (>20 mm long) plant and wood fibres have been considered. As per our knowledge, bio-based naturally-constructed, or even pre-constructed, macro-balloon fillers have not been explored thus far. We proposed that cocoon shells, such as those of domesticated *Bombyx mori* and wild *Gonometa postica* silkworms, offer various advantages over conventional particulate fillers, particularly polymeric microspheres in syntactic foams.

By investigating novel syntactic bio-foams based on a bio-polyurethane matrix and natural silkworm cocoons fillers, we have shown that silk cocoons can be employed as innovative volume-occupying reinforcements in polymer foams to facilitate i) property enhancement, ii) cost reductions, and iii) transitions into sustainable material technologies.

We characterised the physical, mechanical, thermal and environmental resistance properties of the cast bio-foams. Replacing a substantial quantity (60–90% by weight and 40–70% by volume) of the polymer matrix, the low-cost and sustainable silk cocoons of both domesticated and wild silkworms increased the density of the unreinforced foam from 45 kg/m³ to ~60 kg/m³ and ~120 kg/m³ respectively, but also offered a marked increase in both absolute and specific compressive properties. For instance, foams incorporating wild silk cocoons had absolute (657 ± 47 kPa) and specific ($5.5\text{--}6.1$ kPa/(kg/m³)) strength 230% and 15% higher than that of the unreinforced polyurethane foam. An Ashby plot was generated to evaluate the mechanical properties of the novel cocoon reinforced bio-foams against conventional cellular materials, demonstrating that the former were comparable to very low density (18–37 kg/m³) rigid polymer foams.

Key insights of our study particularly demonstrate the viability of silk cocoons as natural particulate reinforcements. The prolate spheroid shape of the cocoon not only enables high filler fractions in a cast processing technique, but also imparts the foam with anisotropic properties. If the anisotropy is aligned in the principal loading direction, for instance perpendicular to the surface in a crash helmet, the high specific properties of the cocoon reinforced bio-foams can be effectively utilised. Attractively, the non-woven laminate structure of the silk cocoons imparts a gradual damage mechanism, eliminating the typical collapse plateau in the stress-strain curve of an unreinforced foam, to the resulting syntactic foam. Finally, the comparable thermal and dimensional stability of the proteinaceous cocoon reinforced polymer foam with the unreinforced polymer foam attest to comparable environmental resistance.

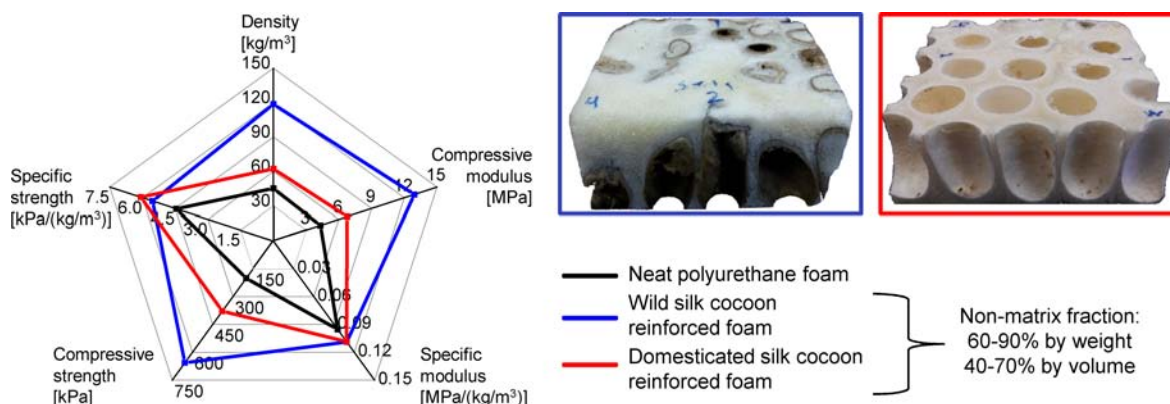


Figure 3.14 Syntactic bio-foams employing silkworm cocoons as volume-occupying fillers.

To take this work further, this year, we will investigate novel silk-based sandwich-structured composites employing woven silk/epoxy laminate skins and a cocoon reinforced bio-foam core.

Evaluating sustainability of silk and its composites

Sustainability of materials and production processes is becoming ever more important for human industry and commerce. Nature's silks are well placed to provide relevant and generic insights. Upon comparison with a typical polymer (high density

polyethylene), silk feedstock is shown to require 1000 times less total energy in order to generate fibrils. We have previously proposed that Nature achieves this massive energy saving by employing a specific type of material, an “aquamelt.” An aquamelt is a naturally hydrated polymeric material that is able to solidify at environmental temperatures/pressures as a result of a controlled stress input perhaps enhanced by a subtle chemical contribution. It is our opinion that using aquamelts as a source of bioinspiration may also help uncover new ways to manipulate hydrogen bonding during processing in both biological (e.g., collagens or celluloses) and synthetic polymers and access Nature’s low energy processing routes.

Nonetheless, given that silk fibre is produced on a large commercial scale today, exclusively for textiel garment applicaitons, but as our studies propose, potentially for reinforced composites applications, we are very active in the research of quantifying envrionemntal impact through a cradle-to-gate assessment of silk fibre production. Over the past year, we have constructed the first ever ife cycle inventory of the production of silk, through a case-study of silk farmers and producers in Karnataka, India. Carrying out analyses as per standards (ISO14040/44), we constructed models of mulberry cultivation, silkworm rearing, and silk reeling. We quantified the following environmental impact indicators: global warming potential, ecotoxicity, freshwater eutrophication, land occupation, cumulative energy demand and blue water footprint. The analysis compares best practice recommendations with observed farm practices. Where applicable, data gaps have been highlighted.

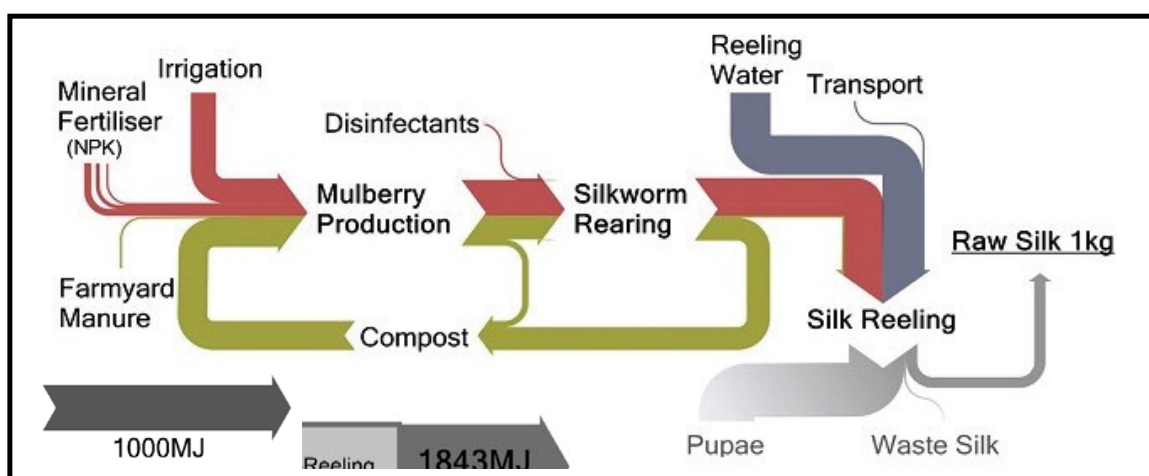


Figure 3.15 Life cycle assessment of silk production.

Our results indicate that silk production, following recommended practices, is input intensive and that on a mass basis environmental impacts are above those reported for other natural fibres like cotton and flax. The majority of environmental impacts stem from cocoon production, in particular fertilization. Farm practices diverge from recommendations significantly and the observed impact per functional unit is higher. The multiple stages required to manufacture raw silk result in a large amount of co-products. Increasing the efficiency in utilisation of these could reduce the high impact observed in this study.

However, it is important to mention that socio-economic aspects, such as job creation, also need to be considered as natural fibres are agricultural fibres with notable benefit for the fibre crop growers and their communities. Consequently, we are developing a new methodology (namely, Eco-SWOT), which conducts a more honest and broader evaluation of the impact of silk production.

So far, we have evaluated the energy demand of silk fibre production. In the next year, we will look to assess the environmental impact of a silk reinforced green composite (i.e. bio-based matrix). Factors such as design life of a component may have a significant impact on the overall performance of silk composites relative to other conventional materials.

Applications for developed silk material technologies

Our work on biological engineering materials ranges from fundamental studies right through to applications of the developed material technologies.

To demonstrate the ability to produce 3D complex shaped silk textile composite parts using conventional manufacturing processes (specifically, vacuum bagging), we have built the composite shell ($v_f = 30\%$) of a crash helmet. Both the part and the mould for the part were fabricated in-house. The silk helmet has a mass of 230g, which would be about 30% lower than a similar composition glass reinforced helmet. The component also acts as a generic prototype for an advanced, eco-structural silk-composite-based bicycle/activity helmet that we will be codeveloping with Dr HA Riina (NYU Neurosurgery) in the 3rd year. The novel helmet will specifically incorporate dedicated mechanisms to protect against common oblique-impact related head rotation and consequent injuries to the brain; an aspect that current helmets are not designed for.



Figure 3.16 Prototype parts made at the Oxford Silk Group: silk reinforced composite outer shell of a crash helmet.

In May 2014, Prof David Porter attended the BioSoar meeting in Seattle, and contributed as an expert in engineering biomaterials. Alongside the manufacture of rigid composites with silk reinforced thermosets, we have also been conducting preliminary studies on the development of soft composites with silk reinforced natural rubbers. In the 3rd year, we will be collaborating (including a secondment) with the Kasetsart Agricultural and Agro-Industrial Product Improvement Institute (Kasetsart University, Thailand) on developing silk reinforced natural rubber composites. The work will also include reverse-engineering the famous Olympic bicycle tire casings made from silk/latex. Such soft, compliant silk composites may find particularly useful applications in soft robotics and UAVs, where a strong balance between light weight, high toughness and high compliance is required. Over the past year, we have briefly worked on the development of inflatable silk/latex tubes for lifting hospital patients. For UAV design, we are proposing the use of tensairity-type morphing wings with inflatable silk/latex sleeves.

Summary, timeliness and potential benefits of the research project

Spider silk is spun from an aqueous solution at ambient pressures and temperatures, and can easily be recycled. This understanding underpins all of our research, which thus commercially responds to recommendations for the improvement of existing materials and processes, especially on weight-saving (as well as bio-compatible) technologies for specific applications. Special importance derives from our materials complying with environmental pressures and legislation and the increasingly demands for recyclable and reusable materials and clean manufacturing processes.

Of course, potential end-users must have confidence in silk as a reliable structural or functional material. To achieve this important goal, fundamental research needs to establish solid understanding of issues such as variability and quality that currently hinder the use of natural silk materials in many applications.

Producing silks requires sustainable implementations of the spinning or extrusion processes that convert aqueous protein feedstock into solid polymeric material with outstanding and predictable mechanical properties. Inter alia this necessitates a solid understanding also of relevant features of feedstock chemistry, which can be elucidated only by rheological and thermal analysis studies.

Finally, exploitation of all the potential advantages of silk's strengths and toughnesses, fabrication route must be found to assemble the natural fibres into sustainable engineering structures. Key will be the interaction of fibre and matrix materials. Hence the search for resins appropriate to our fibres could well be the key to a future for silks in engineering applications.

Design and Development of silk based man-made composites

As we have shown, silks represent a unique family of structural proteins offering a wide range of properties that could be very useful for composite materials i.e. materials/products that combine silks with other materials. The environmental stability, biocompatibility, biodegradability, good mechanical properties and competitive pricing make seem silks interesting candidates for integration into complex composites.

As an engineering fibre with an attractive combination of strength and toughness, natural *B. mori* silk fibres are important candidate reinforcements for polymer composites. Indeed, within the AFSOR grant, we have previously studied natural silkworm cocoons as a model for synthetic nonwoven composites. To date, much research on natural (as opposed to regenerate) silk fibre composites focuses on utilising three reinforcements forms: short fibre reinforcements, waste fabric, and textile fabrics (for instance, woven fabrics). In addition, the matrix phase is either a biodegradable plastic (typically for biomedical applications), or conventional resins (such as epoxies) that are typically used with brittle synthetic fibres (like E-glass and carbon). Importantly, short fibre reinforcements are ineffective in transferring the unique properties of silk fibres to the composite, due to the fibre length being comparable to the critical fibre length; consequently, the composite properties are only marginally improved, in comparison to the neat matrix. Textile fabrics, which are conventional preforms for high-performance composites, are more suitable for load-bearing composites applications. Regarding the choice of matrix, biodegradable resins such as PLA and PBS have inherently low mechanical properties (due to the non-cross-linked nature of the thermoplastic material) implying that the resulting composite mechanical properties are limited. On the other hand, traditional high-performance thermoset matrices (like polyesters and epoxies) have a lower failure strain than the silk fibres, implying that the fracture mechanics of the system is unfavourable. Some researchers have expressed concern over the low packing-ability of silk preforms and impregnation-related issues in producing composites.

Current Status: So far, we have focussed on (i) carrying out a thorough literature review on the use of silks in reinforced plastics, (ii) sensibly selecting and sourcing materials (including polymer matrices and silk reinforcement products) and developing a well-thought out design of experiments (DOE), (iii) learning key techniques and developing standard operating procedures (SOPs) in the characterisation of composite properties, and (iv) conducting preliminary studies on the manufacture and characterisation of silk composites.

As silk reinforcing materials, we have selected five varieties of high-quality Italian woven textile silk fabrics. These will allow studying the effect of (i) textile architecture (i.e. plain weave versus twill weave), (ii) ply orientation (i.e. [0,90] versus $[\pm 45]$, and warp versus weft direction), (iii) silk fabric 'quality' (i.e. organza versus crepe fabric), (iv) and fibre surface treatment (i.e. raw versus degummed fabrics), on composite thermo-mechanical properties. For comparative studies, plain weave textile fabrics of European flax and hemp have also been sourced. As matrix materials we have looked to select resins that are likely to be compatible with silk. Our matrix selection criteria was, (i) high failure strain (\geq failure strain of silk i.e. 10-15%), (ii) low processing viscosity (< 800 cPs at 30°C), (iii) low processing temperatures ($<$ degradation temperature of silk fibres, but typically ambient curing systems requiring up to 100°C post cure), and (iv) high toughness properties. We have been able to source i), (ii) high failure strain epoxies from Momentive (EPIKOTE RIM-R135) and Alchemie (ALCHEMIX EP 5300), (iii) an elastomeric polyurethane from Alchemie (ALCHEMIX PU 3525), and (iv) a cashew-nut seed oil based polyurethane from Elmira, as the resins to be used in this study.

As part of the DOE and to develop an SOP, we have conducted FTIR and thermogravimetric analyses on the different fabric reinforcements to identify and study differences in the FTIR spectra and thermal degradation behaviour. For instance, the TGA analysis reveals that the silk fabrics have distinct (and very repeatable) thermal degradation behaviours, and the processing of the silk fibre has a slight but noticeable effect (In particular, it is observed that degummed silk fabrics have a better thermal stability than raw silk fabrics, and raw silk fabrics show up to 5 wt% higher residual weights than degummed silk fabrics. Typically, silk fabrics start to decompose at about 250°C . This is consistent with control experiments carried out on samples of raw silk and degummed silk from *B. mori* cocoons. In comparison, although flax and hemp fabrics have similar weight loss (up to 10%) due to moisture loss and similar thermal degradation initiation temperatures to the silk fabrics, the plant fibre fabrics degrade more rapidly, stabilising at about 500°C at a lower residual weight of 10-15 wt%.

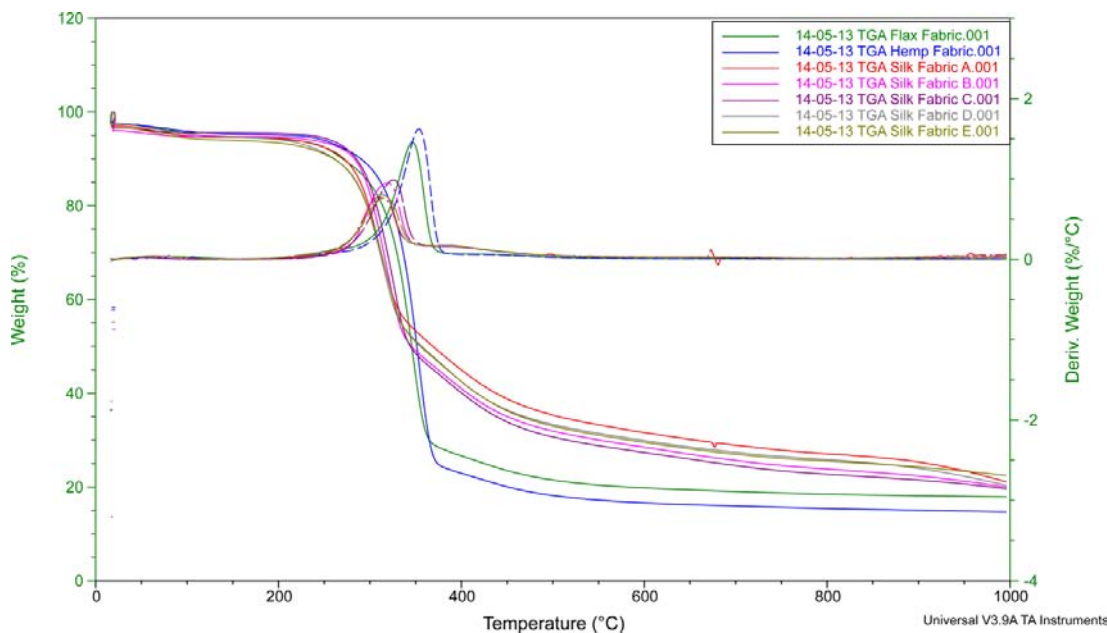


Figure 3.17 TGA curves of various silk and plant fibre woven fabrics. ~5 mg samples were heated from 25°C to 1000°C at a heating rate of $10^\circ\text{C}/\text{min}$, in an inert atmosphere (N_2 gas flow rate of $100\text{ mL}/\text{min}$). Changes in weight percentage during temperature scanning and the decomposition temperatures of the materials can be determined. Silks fabrics of different qualities (Silk Fabric A – E) have distinct (and very repeatable) thermal degradation behaviours. Plant fibre fabrics (flax and hemp) have similar thermal degradation initiation temperatures to the silk fabrics (at about 250°C), but degrade more rapidly with lower residues.

The same SOP will be used in the characterisation of composite and matrix properties as well, enabling a systematic study on the effect of embedding silk fibres in a matrix material to produce a heterogeneous composite.

We have also conducted successful preliminary tests on manufacturing silk/epoxy composites. This produced composites, with a nominal fibre volume fraction of 29.4 ± 1.0 % (fibre weight fraction of 31.9 ± 1.1 %), using a hand lay-up technique. From visual inspection, the composites have low void content (<5 v/v%) confirming our hypothesis that using liquid resin systems with low mixed viscosities will be beneficial in producing low-void content composites (as porosity has a significant detrimental effect on composite properties) with useful fibre volume fractions. To minimise the void content further and to improve preform wettability, we have designed and manufactured in-house a re-useable aluminium mould tool that will be suitable in producing composite laminates (in various pre-defined thicknesses) via both, vacuum infusion and resin transfer moulding. This will then allow the comparison of the mechanical properties of silk composites manufacture using at least two different manufacturing processes.

For initial testing, we have run an FTIR and TGA analysis on the composite specimen. Fig 3.7 shows the TGA profiles of the reinforcing silk fabric, the neat epoxy resin, and the silk/epoxy composite. It is observed that the silk/composite lacks the initial weight loss due to moisture loss of the silk fabric. Rather, the silk/composite shows a slow gradual weight loss up to 250 °C, possibly due to moisture loss or plasticisation of the matrix due to the presence of moisture. Employing silk fibres in the composite reduces the thermal stability of the matrix, but increases the residual weight. It is interesting to observe that silk fibre embedded in the matrix seems to shield/avoid the double peak in the derivative weight loss. We also note that the thermal degradation profile of the composite above 300 °C matches that of the matrix. The relative residual weights of the fibre, matrix and composite can be used to determine the fibre weight fraction of a composite (which is in agreement with the initially measured fibre weight fraction of ~ 31 wt%); it is useful to note that the repeatability of the TGA curves indicates that the composite manufacturing process utilised ensures uniform fibre distribution.

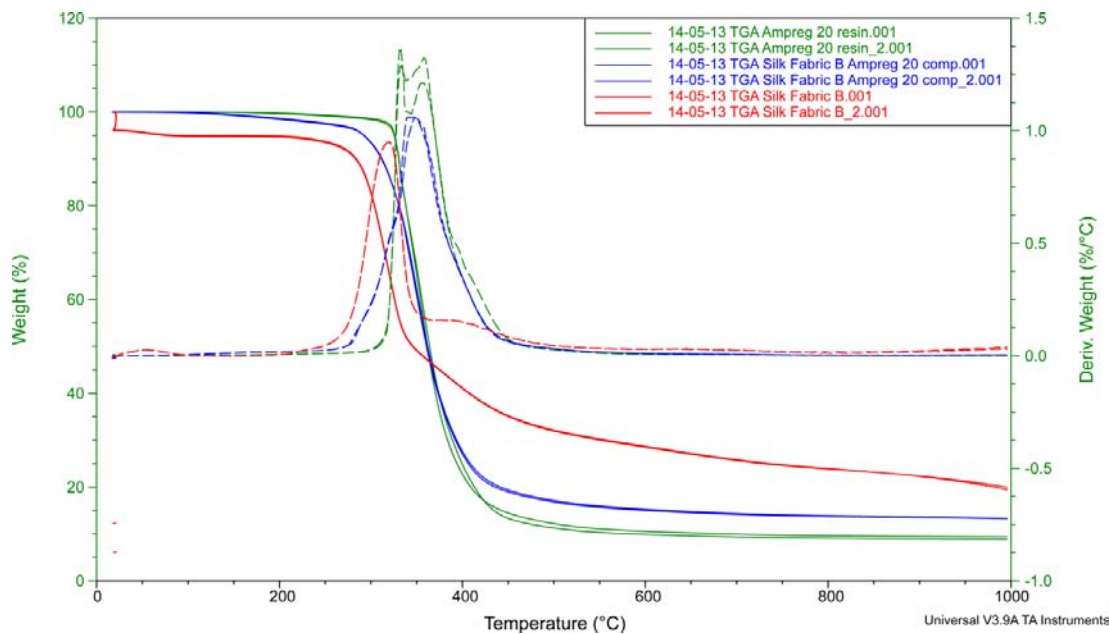


Figure 3.18 TGA curves of silk fabric, neat epoxy resin, and silk/epoxy composite. Similar testing parameters to TGA samples . The curve of the silk/epoxy composite lies in between the curve of the fibre and the matrix, showing the effect of the fibre on the thermal degradation of the reinforced matrix. Specifically, it is

observed that although silk/composites have a lower thermal degradation initiation temperature than the neat matrix, the former have a lower-magnitude single-peaked derivative weight loss.

We have also run thermo-mechanical tests on the initial silk/epoxy specimen, using a DMTA in single cantilever and double cantilever modes. This has enabled us to set-up an SOP for testing the other composites. Our initial results from the DMTA (Fig 3.7) show that the flexural stiffness of the woven silk composites at ambient conditions is comparable to the of the matrix (at ~3 GPa). Notably, this is higher than the stiffness of woven jute/polyester composites with a fibre weight fraction of 27% (similar to our silk composites), which ranges between 1.1 to 2.7 GPa (also measured on a DMTA in single cantilever mode) [9]. The Tg of the resin is estimated to be 80-90 °C, which is in agreement with datasheet values.

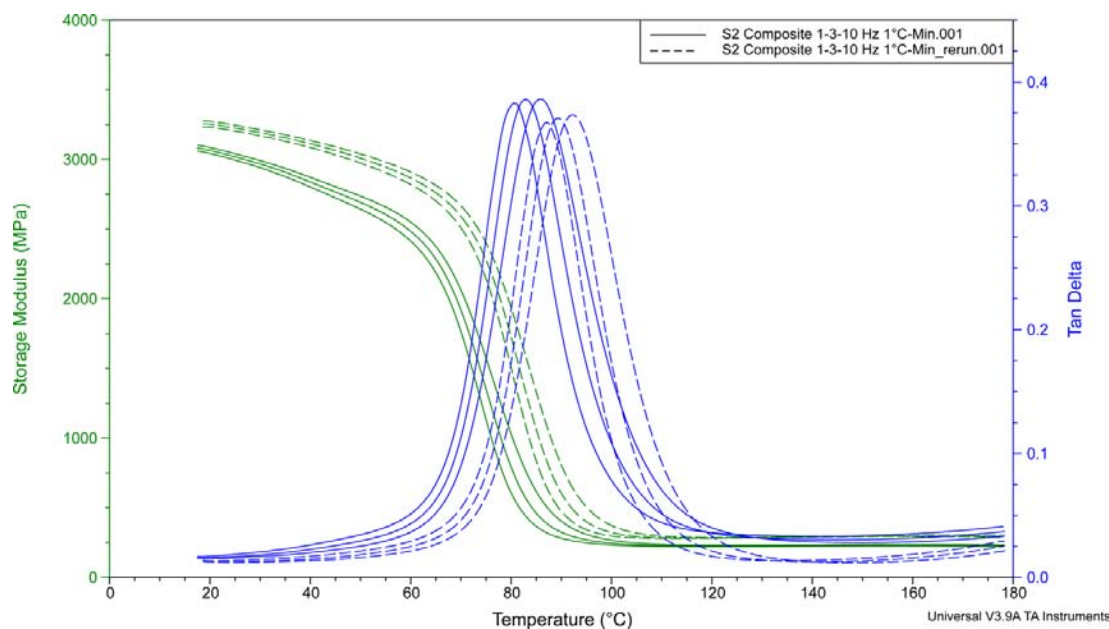


Figure 3.19 Viscoelastic properties of silk/epoxy composites tested using a DMTA, in single cantilever mode, over a range of temperatures (20 °C to 180 °C, at a heating rate of 1 °C/min) and frequencies (from left to right, 1, 3 and 10 Hz). The solid line is a first run of the sample, and the dashed line is a re-run of the same sample; the latter enables studying the effect of aggressive post-cure. Conducting tests at different frequencies (1, 3 and 10 Hz) allows us to study frequency-temperature effects; increasing frequency shifts all the curves to the right, leading to improved storage modulus (at a given temperature) and higher glass transition temperature.

Finally, we discussed possible techniques to measure the interfacial shear strength (IFSS) and interlaminar shear strength (ILSS) of the fibre matrix interface and composite, respectively. Both give an estimate of the interfacial properties, but at a micro- and macro-scale respectively. For ILSS measurement, which is more representative of interfacial properties in a real composite, we have selected the use of Isopescu (v-notch) test and 10° tensile test. For IFSS measurement, due to the thin (and variable) silk fibre diameter and the small estimated critical fibre lengths of the order of 100-200 µm (for interfacial shear strength of 15 MPa – testing would require forces of 30-100 mN), we have decided to conduct a microbond pull-out test, based on accurately determining the embedded length in the matrix post-testing.

Summary, timeliness and potential benefits of the research project

Spider silk is spun from an aqueous solution at ambient pressures and temperatures, and can easily be recycled. This understanding underpins all of our research, which thus commercially responds to recommendations for the improvement of existing materials and processes, especially on weight-saving (as well as bio-compatible) technologies for specific applications. Special importance derives from our materials complying with environmental pressures and legislation and the increasingly demands for recyclable and reusable materials and clean manufacturing processes.

Of course, potential end-users must have confidence in silk as a reliable structural or functional material. To achieve this important goal, fundamental research needs to establish solid understanding of issues such as variability and quality that currently hinder the use of natural silk materials in many applications.

Producing silks requires sustainable implementations of the spinning or extrusion processes that convert aqueous protein feedstock into solid polymeric material with outstanding and predictable mechanical properties. Inter alia this necessitates a solid understanding also of relevant features of feedstock chemistry, which can be elucidated only by rheological and thermal analysis studies.

Finally, exploitation of all the potential advantages of silk's strengths and toughnesses, fabrication route must be found to assemble the natural fibres into sustainable engineering structures. Key will be the interaction of fibre and matrix materials. Hence the search for resins appropriate to our fibres could well be the key to a future for silks in engineering applications.

Interactions, Awards etc

Fritz Vollrath, Chris Holland and David Porter Fritz Vollrath had a great number of discussions as well as lab visits with fellow researchers. Chris Holland was awarded a prestigious EPSRC career Advancement grant as well as a lectureship in the Materials Department at Sheffield University. Darshil Shah was awarded his PhD and Tom Gheysens accepted a tenured position at the European Space Agency. *We note with great sadness that David died suddenly and unexpectedly on June 3rd from a congenital heart condition that manifested itself for the first time at the BioSoar Seattle meeting.*

List of interactions relevant to this award.

- Jeff Urbach and Dan Blair (*Georgetown University Washington DC*) on silk rheology
- Dimitry Deheys (*Scripps and UCSD*) visit Oxford, on tube worm tube composite structure
- Matthew Shawkey (*University of Akron*) on hair structure/function
- Tara Sutherland (*CSIRO, Canberra*) on hymenopteran helical silks
- Larry Drummy (*AFRL, WPAFB*) on ionic liquid effects on silk reconstitution;
- Paul Truelove (*USNA*) visit Oxford, laser annealing
- Tony Ryan and Sasha Mykhaylyk (*Sheffield University*) on silk and polymer rheology
- Hannes Schniepp (*William & Mary College, Virginia*) on AFM microscopy
- Ann Terry (*ISIS, Harwell*) and Thilo Seidel (*ILL, Grenoble*) on Neutron Scattering
- Imke Greving (*DAISY, Hamburg*) on silk tomography
- Zhengzong Shao (*Fudan University, Shanghai*) on silk structure-properties;
- Kathy Wahl (*U.S. Naval Research Laboratory, Washington D.C.*) on silk-film tribology;
- Oxford Biomaterials Ltd (*Oxford*) on silks for tissue scaffolds

All members of the team funded by the AFOSR gave a number of invited keynote lectures as well as engaging in a considerable number of interactions with the public ranging from TV and radio interviews, major exposure in main news papers and lectures for the public.

Publications acknowledging AFOSR support during award period (Yr 3 again in grey)

2015 Boulet-Audet M., Vollrath F., & Holland C. - Identification and classification of silks using infrared spectroscopy. *J. Exp. Biol.*, in press

2015 Astudillo, M.F., Thalwitz, G. & Vollrath, F. - Life cycle assessment of Indian silk. *Journal of Cleaner Production*. In press

2015 Mortimer, B., Guan, J., Holland, C., Porter, D., & Vollrath, F. - Linking naturally and unnaturally spun silks through the forced reeling of *Bombyx mori*. *Acta Biomaterialia*, 11: 247-255

2014 Shah, D.U., Porter, D. & Vollrath, F. - Silk cocoons as natural macro-balloon fillers in novel polyurethane-based syntactic foams. *Polymer* 56: 93–101

2014 Shah, D.U., Porter, D. & Vollrath, F. - Can silk become an effective reinforcing fibre? A property comparison with flax and glass reinforced composites. *Composites Science and Technology*, 101: 173-183.

2014 Vollrath, F., Hawkins, N., Porter, D., Holland, C. & Boulet-Audet, M. - Differential Scanning Fluorimetry provides high throughput data on silk protein transitions. *Scientific Reports*, 4: 5625.

2014 Shah, D.U., Vollrath, F., Porter, D., Stires, J. & Deheyn D.D. - Housing tubes from the marine worm, *Chaetopterus* sp.: biomaterials with exceptionally broad thermo-mechanical properties. *Journal of Royal Society Interface*, 11(98): 20140525.

2014 Mortimer, B., Gordon, S.D., Holland, C., Siviour, C.R., Vollrath, F., & Windmill, J.F. - The speed of sound in silk: Linking material performance to biological function. *Advanced Materials*.

2014 Shah, D.U. - Natural fibre composites: Comprehensive Ashby-type materials selection charts. *Materials and Design*, 62: 21-31.

2014 Shah, D.U., Vollrath, F. & Porter, D. - Opportunities for silk textiles in reinforced biocomposites: Studying through-thickness compaction behaviour. *Composites Part A: Applied Science and Manufacturing*, 62: 1-10.

2014 Boulet-Audet, M., Terry, A., Vollrath, F. & Holland, C. - Silk protein aggregation kinetics revealed by Rheo-IR. *Acta Biomaterialia*, 10 (2): 776-784

2013 Vollrath, F. & Edmonds, D. - Consequences of Electrical Conductivity in an Orb Spider's Capture Web. *Naturwissenschaften*, 100 (12): 1163-1169

2013 Bauer, G., Friedrich, C., Gillig, C., Vollrath, F., Speck, T. & Holland, C. - Investigating the rheological properties of native plant latex. *J. R. Soc. Interface*, 11: 20130847

- 2013 Guan, J., Vollrath, F. & Porter, D. - Silk quality revealed using Dynamic Mechanical Thermal Analysis (DMTA). in '6th BACSA International Conference: Building Value Chains in Sericulture'. Padua, Italy.
- 2013 Vollrath, F., Carter, R., Rajesh G.K., Thalwitz, G. & Astudillo, M.F. - Life Cycle Analysis of Cumulative Energy Demand on Sericulture in Karnataka, India. in '6th BACSA International Conference: Building Value Chains in Sericulture'. Padua, Italy.
- 2013 Wang, Y., Porter, D. & Shao, Z. - Using Solvents with Different Molecular Sizes to Investigate the Structure of *Antheraea Pernyi* Silk. *Biomacromolecules*, 14 (11): 3936-3942
- 2013 Mortimer, B., Holland, C. & Vollrath, F. - Forced Reeling of *Bombyx mori* Silk: Separating Behavior and Processing Conditions. *Biomacromolecules*, 14 (10): 3653-3659
- 2013 Davies, G.J.G., Knight, D.P. & Vollrath, F. - Chitin in the Silk Gland Ducts of the Spider *Nephila edulis* and the Silkworm *Bombyx mori*. *PLOS ONE*, 8 (8): e73225
- 2013 Shah, D.U. - Developing plant fibre composites for structural applications by optimising composite parameters: a critical review. *Journal of Materials Science*, 48 (18): 6083-6107
- 2013 Davies, G.J.G., Knight, D.P. & Vollrath, F. - Structure and function of the major ampullate spinning duct of the golden orb weaver, *Nephila edulis*. *Tissue and Cell*, 45 (5): 306-311
- 2013 Guan, J., Porter, D. & Vollrath, F. - Thermally Induced Changes in Dynamic Mechanical Properties of Native Silks. *Biomacromolecules*, 14 (3): 930-937
- 2013 Mortimer, B., Drodge, D.R., Dragnevski, K.I., Siviour, C.R. & Holland, C. - In situ tensile tests of single silk fibres in an environmental scanning electron microscope (ESEM). *Journal of Materials Science*, 48 (14): 5055-5062
- 2013 Horrocks, N.P.C., Vollrath, F. & Dicko, C. - The silkmoth cocoon as humidity trap and waterproof barrier. *Comp Biochem Physiol A Mol Integr Physiol.*, 164 (4): 645-652
- 2013 Vollrath, F., Porter, D. & Holland, C. - The Science Of Silks. *MRS Bulletin*, 38 (1): 73-80
- 2013 Porter, D. & Vollrath, F. - Water mediated proton hopping empowers proteins. *Softmatter*, 9 (3): 643-646
- 2013 Porter, D., Guan, J. & Vollrath, F. - Spider Silk: super material or thin fibre? *Advanced Materials*, 25 (9): 1275-1279
- 2012 Yang, Y., Dicko, C., Bain, C.D., Gong, Z., Jacobs, R.M.J., Shao, Z., Terry, A.E. & Vollrath, F. - Behavior of silk protein at the air–water interface. *Soft Matter*, 8 (37): 9705-9712
- 2012 Hesselberg, T. & Vollrath, F. - The mechanical properties of the non-sticky spiral in *Nephila* orb webs (Araneae, Nephilidae). *J. Exp. Biol.*, 215 (19): 3362-3369

- 2012 Drodge, D.R., Mortimer, B., Holland, C. & Siviour, C.R. - Ballistic Impact to Access the High-Rate Behaviour of Individual Silk Fibres. *Journal of the Mechanics and Physics of Solids*, 60 (10): 1710-1721
- 2012 Chen, F., Porter, D. & Vollrath, F. - Structure and physical properties of silkworm cocoons. *Journal of the Royal Society Interface*, 9 (74): 2299-2308
- 2012 Porter, D. & Vollrath, F. - Water mobility, denaturation and the glass transition in proteins. *Biochimica et Biophysica Acta (BBA) - Proteins & Proteomics*, 1824 (6): 785-791
- 2012 Wang, T., Porter, D. & Shao, Z. - The Intrinsic Ability of Silk Fibroin to Direct the Formation of Diverse Aragonite Aggregates. *Advanced Functional Materials*, 22 (2): 435-441
- 2012 Guan, J., Porter, D. & Vollrath, F. - Silks cope with stress by tuning their mechanical properties under load. *Polymer*, 53 (13): 2717-2726
- 2012 Chen, F., Porter, D. & Vollrath, F. - Silk Cocoon: Multilayer structure and mechanical properties (*Bombyx mori*). *Acta Biomaterialia*, 8 (7): 2620-2627
- 2012 Chen, F. J., Porter, D. & Vollrath, F. - Morphology and structure of silkworm cocoons. *Materials Science & Engineering C-Materials for Biological Applications*, 32 (4): 772-778
- 2012 Kronenberger, K., Moore, P.G., Halcrow, K. & Vollrath, F. - Spinning a marine silk for the purpose of tube-building. *Journal Of Crustacean Biology*, 32 (2): 191-201
- 2012 Holland, C., Vollrath, F. & Dicko, I.C. - Distinct structural and optical regimes in natural silk spinning. *Biopolymers*, 97 (6): 368-73
- 2012 Holland, C., Urbach, J. & Blair, D. - Direct Visualization of Shear Dependent Silk Fibrillogenesis. *Soft Matter*, 8 (9): 2590-4
- 2012 Holland, C., Porter, D. & Vollrath, F. - Comparing the rheology of mulberry and 'wild' silkworm spinning dopes. *Biopolymers*, 97 (6): 362-7
- 2012 Holland, C., Vollrath, F., Ryan, A.J. & Mykhaylyk, O.O. - Silk and Synthetic Polymers; Reconciling 100 Degrees of Separation. *Advanced Materials*, 24 (1): 105-109
- 2012 Greving, I., Cai, F., Vollrath, F. & Schniepp, H. - Shear-induced self-assembly of native silk proteins into fibrils studied by atomic force microscopy. *Biomacromolecules*, 13 (3): 676-682
- 2012 Huang, W., Begum, R., Barber, T., Ibba, V., Tee, N.C., Hussain, M., Arastoo, M., Yang, Q., Robson, L.G., Lesage, S., Gheysens, T., Skaer, N.J., Knight, D.P. & Priestley, J.V. - Regenerative potential of silk conduits in repair of peripheral nerve injury in adult rats. *Biomaterials*, 33 (1): 59-71